JPET Fast Forward. Published on February 24, 2020 as DOI: 10.1124/jpet.119.263483
This article has not been copyedited and formatted. The final version may differ from this version.

JPET# 263483

Title Page

Pharmacological characterization of the novel and selective α7 nicotinic acetylcholine receptor positive allosteric modulator BNC375

Xiaohai Wang[1], Christopher Daley[1], Vanita Gakhar[1], Henry Lange[1], Joshua D. Vardigan[1], Michelle Pearson[1], Xiaoping Zhou[1], Lee Warren[1], Corin O. Miller[1], Michelle Belden[1], Andrew J. Harvey[2, 3], Anton A. Grishin[2], Carolyn J. Coles[2], Susan M. O'Connor[2], Fiona Thomson[1, 4], Joseph L. Duffy[1], Ian M. Bell[1], Jason M. Uslaner[1]

1. Merck & Co., Inc., 2015 Galloping Hill Road, Kenilworth, NJ 07033, USA
2. Bionomics Limited, 31 Dalgleish Street, Thebarton, SA-5031, Australia
3. Current address: UniQuest Pty Ltd., Level 7, General Purpose South Building, Staff House Road, Brisbane, QLD-4072, Australia
4. Current address: Institute of Cancer Sciences, University of Glasgow, Glasgow G61 1QH, UK

JPET# 263483

Running Title page

Pharmacological characterization of the α7 nAChR PAM BNC375

Corresponding author:

Xiaohai Wang

Department of Neuroscience Research, Merck & Co., Inc.,

770 Sumneytown Pike, WP14-3393, West Point, PA 19486

Tel: 215-6521085

Email: xiaohai_wang@merck.com

Number of text pages: 58

Tables: 1

Figures: 10

References: 63

Words in the Abstract: 249

Words in the Introduction: 754

Words in the Discussion: 1735

Abbreviations: ACh, acetylcholine; aCSF, artificial cerebrospinal fluid; AD, Alzheimer's disease; AGM, African green monkey; AUC, area under curve; fEPSP, field excitatory postsynaptic potentials; LTP long-term potentiation; MLA, methyllycaconitine; mPFC, medial prefrontal cortex; nAChR, nicotinic acetylcholine receptor; ORD, object retrieval detour; PAM, positive allosteric modulator; TBS, theta-burst stimulation;

Recommended section assignment: Neuropharmacology

Abstract

Treatments for cognitive deficits associated with CNS disorders such as Alzheimer's disease (AD) and schizophrenia remain significant unmet medical needs that incur substantial pressure on the healthcare system. The α7 nicotinic acetylcholine receptor (nAChR) has garnered substantial attention as a target for cognitive deficits based on receptor localization, robust preclinical effects, genetics implicating its involvement in cognitive disorders, and encouraging, albeit mixed clinical data with α7 nAChR orthosteric agonists. Importantly, previous orthosteric agonists at this receptor suffered from off-target activity, receptor desensitization, and an inverted U-shaped dose-effect curve in preclinical assays that limit their clinical utility. To overcome the challenges with orthosteric agonists, we have identified a novel selective α7 positive allosteric modulator (PAM), BNC375. This compound is selective over related receptors and potentiates acetylcholine (ACh)-evoked α7 currents with only marginal effect on the receptor desensitization kinetics. In addition, BNC375 enhances long-term potentiation (LTP) of electrically evoked synaptic responses in rat hippocampal slices and *in vivo*. Systemic administration of BNC375 reverses scopolamine-induced cognitive deficits in rat novel object recognition and rhesus monkey object retrieval detour (ORD) task over a wide range of exposures, showing no evidence of an inverted U-shaped dose-effect curve. The compound also improves performance in the ORD task in aged African green monkeys. Moreover, ex vivo ^{13}C-NMR analysis indicates that BNC375 treatment can enhance neurotransmitter release in rat medial prefrontal cortex. These findings suggest that α7 nAChR PAMs have multiple advantages over orthosteric α7 nAChR agonists for the treatment of cognitive dysfunction associated with CNS diseases.

Significance Statement

BNC375 is a novel and selective α7 nAChR PAM that potentiates ACh-evoked α7 currents in in vitro assays with little to no effect on the desensitization kinetics. In vivo, BNC375 demonstrated robust procognitive effects in multiple preclinical models across a wide exposure range. These results suggest that α7 nAChR PAMs have therapeutic potential in CNS diseases with cognitive impairments.

Introduction

Accumulating evidence suggests that the α7 nicotinic acetylcholine receptor (nAChR) may play an essential role in cognitive performance. In the central nervous system (CNS), the α7 nAChR is highly expressed in hippocampus, cerebral cortex, and thalamus, brain regions involved in cognitive function, and activation of α7 nAChR has been shown to modulate synaptic function and influence the release of a variety of neurotransmitters, such as glutamate, γ-aminobutyric acid (GABA), ACh, norepinephrine, and dopamine (Livingstone et al., 2009; Huang et al., 2014; Koranda et al., 2014). Preclinical studies in multiple species have demonstrated that enhancing α7 nAChR activity improves cognitive deficits in episodic memory (Sahdeo et al., 2014; Weed et al., 2017), working memory (Ng et al., 2007; Castner et al., 2011), and attention (Pichat et al., 2007; Rezvani et al., 2009), whereas blocking or genetically deleting the receptor is associated with impaired cognitive performance (Keller et al., 2005; Young et al., 2007). Furthermore, the expression level of α7 nAChR can be affected by several pathological conditions, including AD and schizophrenia (Freedman et al., 1995; Guan et al., 2000; Wevers et al., 2000; Kadir et al., 2006). Human genetic evidence indicates that both large deletions to the region of 15q13.3 in chromosome 15 and smaller deletions to the gene for the α7 nAChR, CHRNA7, frequently produce cognitive impairments (Sharp et al., 2008; Le Pichon et al., 2013).

Various strategies have been aimed at pharmacologically enhancing α7 nAChR function to treat cognitive deficits associated with AD and schizophrenia. One such approach has been to develop orthosteric α7 nAChR agonists, which bind to the same site as the endogenous ligand ACh. A variety of α7 full or partial agonists have been developed over

the past two decades (Hurst et al., 2013; Bertrand et al., 2015), and several candidates have advanced into clinical trials for the treatment of cognitive deficits associated schizophrenia and AD. However, despite the strong preclinical evidence and some positive clinical findings, most notably with encenicline demonstrating encouraging results in phase 2 studies for schizophrenia and AD, clinical development of selective α7 agonists has not progressed (Bertrand et al., 2015). It is thought that this has been in large part due to the limitations associated with orthosteric approaches for targeting the α7 nAChR, which include: 1) lack of selectivity resulting in dose-limiting side-effects e.g. serotonin 5-HT3 receptor antagonism; 2) desensitization and loss of function with sustained exposure to agonist; and 3) inverted U-shaped dose-response function which may restrict the efficacy of an α7 agonist to a very specific, narrow range of drug exposure (Deardorff et al., 2015).

Positive allosteric modulators (PAMs) of the α7 nAChR bind to a unique binding site on the receptor and potentiate the effects of the endogenous ligand ACh, and therefore may exhibit an improved clinical profile in comparison to orthosteric α7 agonists. PAMs demonstrate superior selectivity over related Cys-loop superfamily of ligand-gated ion channels through binding to a non-conserved region of the α7 nAChR (Dinklo et al., 2011; Williams et al., 2011) and do not appear to promote receptor desensitization, unlike α7 agonists. Therefore, α7 PAMs may produce efficacy over a wider range of concentrations and maintain efficacy upon repeated dosing. Several structurally distinct α7 PAMs have been identified, and according to their effects on receptor desensitization kinetics, at least two distinct types of PAMs have been described. Type I PAMs, including Compound 6 (AVL-3288), NS1738, and BNC375, potentiate the agonist-induced peak current without

affecting the desensitization kinetics. Type II PAMs, such as PNU120596, RO5126946, JNJ-1930942, and B-973, not only affect peak current but also delay receptor desensitization. So far, only a few α7 PAMs have progressed into clinical evaluation, including JNJ-39393406 which has advanced to phase 2 study for smoking cessation (Perkins et al., 2018) and AVL-3288 which has been evaluated in healthy human subjects for effects on neurocognitive performance (Gee et al., 2017).

Here we characterize the in vitro and in vivo pharmacological properties of a novel and selective α7 nAChR PAM, BNC375. This compound overcomes many of the issues associated with orthosteric agonists. It potentiates α7 currents with Type I-like PAM activity on receptor desensitization kinetics, produces effects in multiple in vivo assays over a broad range of exposures in multiple species, and lacks off-target activity. In addition, consistent with the effects of α7 nAChR activation on neurotransmitter release, we have demonstrated with ex vivo ^{13}C-NMR analysis that BNC375 can promote glutamate cycling and metabolism. This finding allows for a translatable measure of target modulation that could be helpful for dose selection in the clinical trials.

JPET Fast Forward. Published on February 24, 2020 as DOI: 10.1124/jpet.119.263483
This article has not been copyedited and formatted. The final version may differ from this version.

Materials and Methods

Cell Lines

Cell lines were cultured at 37 °C under 5% CO2 in a humidified incubator and dissociated for passaging or electrophysiology assays using Accutase (Innovative Cell Technologies, Inc.). HEK human α7/RIC-3 cells were obtained from Eurofins Inc. and were cultured in DMEM/F-12, 10% fetal bovine serum, 2 mM glutamine, 1% non-essential amino acids, 400 µg/mL Geneticin, 0.625 µg/mL puromycin. TE671 cells were obtained ATCC and cultured in DMEM, 10% fetal calf serum, 10 mM HEPES, 1 mM sodium pyruvate, 2 mM penicillin-streptomycin-glutamine. HEK Human α3β4 cells were from Merck & Co., Inc., Kenilworth, NJ, USA and cultured in DMEM, 6% fetal calf serum, 5 U/mL penicillin, 50 µg/mL streptomycin, 100 µg/mL geneticin, 40 µg/mL zeocin. HEK Human α4β2 cells were from Bionomics Ltd. and cultured in DMEM, 10% fetal calf serum, 10 mM HEPES, 1% non-essential amino acids, 1 mM sodium pyruvate, 600 µg/mL geneticin, 200 µg/mL zeocin. HEK Human $GABA_A$ cells were from Bionomics Limited. and were cultured in DMEM/F-12, 10% fetal calf serum, 10 mM penicillin-streptomycin-glutamine, 2 mM HEPES, 300 µg/mL geneticin. HEK Human 5-HT3a cells were obtained from Bionomics Ltd. and were cultured in DMEM, 10% fetal calf serum, 10 mM HEPES, 1% non-essential amino acids, 1 mM sodium pyruvate, 600 µg/mL geneticin.

IonFlux HT Electrophysiology Assays

The IonFlux HT automated patch-clamp platform (Fluxion Biosciences; Alameda, CA, USA) was used to record ion channel currents from recombinant HEK cell lines stably overexpressing human Cys-loop receptors α3β4, α4β2, α7, $5\text{-}HT3_A$, or $GABA_A$. α1 currents were recorded from TE671 cells where α1 is endogenously expressed.

JPET Fast Forward. Published on February 24, 2020 as DOI: 10.1124/jpet.119.263483
This article has not been copyedited and formatted. The final version may differ from this version.

For α7 assays, extracellular solution was 150 mM NaCl, 5 mM KCl, 2 mM CaCl2, 1 mM MgCl2, 10 mM HEPES, 12 mM dextrose, pH 7.3, and intracellular solution was 110 mM Tris dibasic, 28 mM TrisBase, 0.1 mM CaCl2, 2 mM MgCl2, 11 mM EGTA, 4 mM Mg-ATP, pH 7.3. For α1, α3β4, α4β2, 5-HT3a, and $GABA_A$ assays extracellular solution was 137 mM NaCl, 5 mM KCl, 1.8 mM CaCl2, 2 mM MgCl2, 10 mM HEPES, 10 mM dextrose, pH 7.3, and intracellular solution was 110 mM Tris dibasic, 28 mM TrisBase, 0.1 mM CaCl2, 2 mM MgCl2, 11 mM EGTA, 4 mM Na-ATP, pH 7.3. All patch-clamp recordings were conducted at room temperature in the whole-cell population-patch recording configuration. Following cell capture, seal formation, and achieving whole-cell recording, data were acquired at a holding potential of -60 mV for 5-HT3a, α3β4, α4β2, α7, and $GABA_A$ recordings, and at -80 mV for α1 recordings. Sweep lengths were up to 20 seconds in duration and collected at a rate of 5 kHz to allow for the full capture of channel activation and desensitization kinetics.

BNC375 was prepared as 10 mM stock solutions in dimethyl sulfoxide (DMSO) and diluted manually for α1, α3β4, α4β2, 5-HT3a, and $GABA_A$ assays. For α7 assays, compound titrations were prepared using the Echo acoustic liquid handler (Labcyte Inc.; San Jose, CA, USA) in combination with the Mantis liquid handler (Formulatrix; Bedford, MA, USA) and Bravo liquid handler (Agilent; Santa Clara, CA, USA). The final DMSO concentration was 0.3% in all IonFlux assays. For each patch-clamp recording, a baseline was first established by recording the current response after application of the receptor's natural agonist for 1 second (s): acetylcholine (ACh) for α1, α3β4, α4β2, and α7; 5-hydroxytryptamine (5-HT or serotonin) for 5-HT3a receptor; γ-aminobutyric acid (GABA) for $GABA_A$ receptor. For α7 PAM assays, the EC_{20} of ACh was utilized as it elicited a

consistent current response and resulted in a robust assay window with adequate dynamic range for the detection of PAM activity; for agonist assays, the test compound was applied in the absence of ACh and for PAM assays, the test compound was co-applied with EC_{20} ACh. For α1, α3β4, α4β2, and $GABA_A$ receptor assays, the EC_{40} of ACh or GABA was used as it allowed for simultaneous detection of antagonist and PAM activity. For 5-HT3a receptor assay, the EC_{80} of serotonin was utilized since it resulted in a consistent and robust current response for the detection of antagonist activity. After the baseline current response was established, the cells were pre-incubated with the lowest concentration of BNC375 in a 3-concentration series, for approximately 1 minute. The lowest concentration of BNC375 was then co-applied with agonist for 1 s to detect potentiation or inhibition. The pre-incubation and co-application procedure were then repeated with the second lowest concentration of BNC375, and then finally, the highest concentration of BNC375 in the 3-concentration series. IC_{50} or EC_{50} was derived from the 6-point dose-response curves, where applicable, using standard methods. Agonism, inhibition, and potentiation were calculated as follows, where I_{Test} is the current elicited by the test compound alone, $I_{Control}$ is the current elicited by the control agonist, and $I_{Test + Control}$ is the current elicited by the test compound when co-applied with the control agonist:

$$\% \text{ Agonism} = (I\text{Test}) / (I\text{Control}) \times 100$$

$$\% \text{ Potentiation} = (I\text{Test} + \text{Control}) / (I\text{Control}) \times 100 - 100$$

$$\% \text{ Inhibition} = -((I\text{Test} + \text{Control}) / (I\text{Control}) \times 100) - 100)$$

JPET Fast Forward. Published on February 24, 2020 as DOI: 10.1124/jpet.119.263483
This article has not been copyedited and formatted. The final version may differ from this version.

Whole-cell Patch-Clamp Electrophysiology in GH4C1 Cells

GH4C1 cells stably expressing rat α7 nAChRs were patch-clamped in the recording chamber of 16-channel Dynaflow ReSolve chips using EPC10 USB amplifier (HEKA Elektronik, Germany). Extracellular solution was 137 mM NaCl, 5 mM KCl, 2.5 mM $CaCl_2$, 1 mM $MgCl_2$, 10 mM HEPES, 10 mM D-Glucose, pH 7.4. Thin wall borosilicate glass electrodes (Harvard Apparatus) were pulled to a resistance of 2-4 MΩ when filled with intracellular solution (120 mM K^+-gluconate, 5 mM KCl, 10 mM HEPES, 10 mM EGTA, 1 mM $MgCl_2$, 2 mM ATP, pH 7.2). Cells were held at -70 mV. Cells with series resistance below 15 MΩ were kept and 40% compensation was utilized routinely. The recording protocol consisted of obtaining of two control ACh responses (EC_{20} concentration, 250 ms pulse) prior to 30 s pre-incubation with BNC375 (3 μM) followed by 250 ms co-application of 3 μM BNC375 plus EC_{20} ACh. Dose-response for BNC375 was obtained by a continuous application of BNC375 at increasing concentrations alternated with co--applications of BNC375 plus EC_{20} ACh. The stimulation frequency was one 250 ms co-application pulse per 30 s to ensure complete washout of EC_{20} ACh and full recovery of the α7 receptor from ACh-induced desensitization. Current amplitudes along with net current charge (area under curve, AUC) were measured in a Patchmaster software (HEKA Elektronik, Germany) and percentage of peak current and AUC potentiation by BNC375 was calculated.

Cytotoxicity Assay

GH4C1 cells expressing rat α7 nAChRs were plated on PDL-coated 96-well plates at a density of 10^5 cells/well in complete growth medium containing 500 μM sodium butyrate

and placed into a 33 °C incubator for 48 hours. The medium was then replaced with HBSS containing 10% FBS, 100 μM choline, and appropriate concentrations of compounds. Cells were incubated for an additional 2 hours at 33 °C. Cell viability was determined using a colorimetric 2,3-bis[2-Methoxy-4-nitro-5-sulfophenyl]2H-tetrazolium-5-carboxyanilide (XTT)-based assay (Sigma-Aldrich, Catalog# TOX2). After the 2-hour treatment period, compound solutions were replaced with 100μl fresh HBSS and 20μl/well of XTT (1 mg/ml). Cells were then incubated for another 4 hours at 37 °C, after which absorbance was measured at 450 nm. Cytotoxicity was calculated relative to the cells treated with vehicle.

Animals

Studies were conducted in strict accordance with the National Research Council's Guide for the Care and Use of Laboratory Animals. Protocols were approved by the Institutional Animal Care and Use Committee of Merck & Co., Inc., Kenilworth, NJ, USA.

Hippocampal Slice Preparation

Young adult male Sprague-Dawley rats (Charles River Laboratory) weighing 200-250 g were housed in an air-conditioned room on a 12-hour light/dark cycle with food and water available *ad libitum*. On the day of experiments, animals were terminally anesthetized using isoflurane, cervically dislocated, and decapitated. The brain was removed and 400 μm thick hippocampal slices were cut using a microtome (Leica VT1000S) in ice cold cutting solution (in mM): 93 NMDG, 2.5 KCl, 2.5 NaH_2PO_4, 30 $NaHCO_3$, 20 HEPES, 25 Glucose, 10 $MgSO_4$, 0.5 $CaCl_2$, 5 sodium ascorbate, 2 thiourea, 3 sodium pyruvate. Slices were maintained in standard artificial cerebrospinal fluid (aCSF) at 34 ºC for 10 mins after

slicing. After this period, individual slices were transferred to aCSF for 1 hour at room temperature (17–21°C) and subsequently transferred to a custom-built chamber continuously perfused with aCSF at a rate of 2–4 ml/min. Standard aCSF (in mM): 127 NaCl, 1.9 KCl, 1.2 KH_2PO_4, 2.4 $CaCl_2$, 1.3 $MgCl_2$, 26 $NaHCO_3$, 10 D-glucose, equilibrated with 95% O_2-5% CO_2.

Whole-cell recording in hippocampal interneuron

Whole-cell patch-clamp recordings were performed at room temperature from hippocampal interneurons located in the stratum radiatum with a Multiclamp 700B amplifier. Hippocampal interneurons were visualized on a monitor connected to a Hamamatsu C2400 camera mounted on an Olympus BX51 upright microscope using a 40X water immersion lens. Patch pipettes had resistances of between 3 and 8 MΩ when filled with an intracellular solution of the following composition (in mM): 140 Kgluconate, 10 KCl, 1 EGTA-Na, 10 HEPES, 4 Na_2ATP, 0.3 GTP. Once electrophysiological confirmation of the neuronal subtype had been conducted via a current-clamp current-voltage relationship plot, voltage-clamp experiments (Vh = -60 mV, unless indicated) were carried out in the presence of 2,3-Dioxo-6-nitro-1,2,3,4-tetrahydrobenzo[f]quinoxaline-7-sulfonamide (NBQX, 10 μM), D-(-)-2-Amino-5-phosphonopentanoic acid (D-AP5, 10 μM), Picrotoxin (100 μM), Atropine (5 μM), and dihydro-beta-erythroidine (DhβE, 3 μM) to isolate α7 nAChR-mediated synaptic events. ACh (100 μM, 2-5 secs) was pressure-ejected at low frequency (0.017 Hz) via a picospritzer (NPI PDES-02DX) onto recorded neurons using a glass-barreled electrode positioned ~100 μm from the recorded neuron.

A baseline of at least 5 consecutive responses was obtained before applying the test compound. α7-mediated currents were confirmed by testing sensitivity to the selective antagonist methyllycaconitine citrate (MLA, 1 μM).

Hippocampal slice LTP

After a 1 hour recovery period in the aCSF, individual slices were transferred to a submersion recording chamber and perfused constantly with warmed (30°C) oxygenated aCSF at a flow rate of 2 - 4 ml/min. Schaffer collaterals were stimulated (0.1 ms pulse width, 0.033 Hz) with a concentric bipolar electrode and the evoked extracellular field excitatory postsynaptic potentials (fEPSPs) recorded from the stratum radiatum of the CA1 region of the hippocampus with a glass capillary microelectrode filled with 2 M NaCl (resistance 2-6 MΩ) using an Axoclamp amplifier.

Stimulation parameters were set to produce an fEPSP of approximately 30-40% of the maximum amplitude. A 10-minute stable baseline period (control) was recorded using Axon software (pClamp), followed by administration of test compounds or DMSO control for 15 minutes. The brain slices were then stimulated using a theta-burst stimulation (TBS) protocol for LTP induction (10 mini-trains: 4 pulses, 100Hz, 200 msec apart). The test compound was applied for a further 5 minutes. Experiments with unstable baselines were discarded, whilst in successful experiments fEPSPs were monitored for 60 minutes after LTP induction. All compounds were made as 1000x stock concentrations in DMSO and diluted to the required concentration in aCSF immediately prior to use. Final DMSO concentration was always 0.1% in the slice assay. All compounds were bath applied. All analysis was conducted using Excel (Microsoft) and Clampfit (MDS Technologies).

In vivo LTP

Male Sprague Dawley rats (Charles River Laboratory, 300 – 450 g) were anesthetized initially with isoflurane (5% in oxygen) and subsequently with an intraperitoneal injection of urethane (1 mml/100 g, 12% solution), supplemented as necessary. Core body temperature was monitored and maintained at 37 °C by a homoeothermic blanket system (Harvard Equipment). The left femoral vein and artery, as well as the trachea, were cannulated to permit: (1) administration of supplemental anesthetic; (2) recording of arterial blood pressure via a pressure transducer and amplifier (Neurolog NL108, Digitimer); (3) maintenance of a clear airway. Animals were placed in a stereotaxic frame (Narishige ST-7) and the dorsal brain surface overlying the hippocampus exposed by craniotomy.

Electrodes were lowered vertically through the cortex to the dentate gyrus using the following approximate stereotaxic coordinates. The recording electrode was implanted in the granule cell layer at Bregma -4 mm, lateral +2 mm, 2.5 -3.0 mm below the pial surface. Electrical stimulation (1 ms pulse width, 0.1 Hz) of the performant pathway was made with a coaxial bipolar stainless-steel electrode to evoke field excitatory post-synaptic potential (fEPSP) and superimposed population spike (PS) activity in the dentate gyrus granule cell layer of the hippocampus recorded through an extracellular carbon fiber microelectrode (Kation Scientific). The amplitude of the PS superimposed on the fEPSP was then calculated and presented in real-time. By adjusting the depth of both the stimulating and recording electrode in small increment, the amplitude of the PS was optimized. Thereafter, an input-out curve was generated to determine maximal PS

amplitude and the voltage required to obtain a response with an amplitude of approximately 30-50 % of the maximum.

Stimulation parameters were maintained at 30 – 50 % maximal response at a frequency of 0.033Hz to demonstrate a stable baseline period of at least 10 min before commencing the full experiment protocol. After baseline recording, BNC375 (0.1, 1, or 10 mg/kg, SC) or vehicle (30% Captisol in water) was injected 20 min before induction of LTP. The compound was administered via subcutaneous (SC) route (2 ml/kg). LTP induction parameters: theta burst stimulation (TBS) consists of 5 train of 4 pulses (inter-train interval 170 ms, inter-pulse interval 10 ms). Upon completion of LTP induction, responses were monitored for a further 60 min (Fig 5A). Changes in the amplitude of the PS as calculated as a percentage of control and expressed a mean ± S.E.M.

Rat novel object recognition test

Male Wistar Hannover rats (Charles River Laboratory; n = 7- 11 per group) weighing 200 to 300 g were housed two per cage under reverse12-hour light-dark conditions (lights on 18:00). One hour before testing, animals were brought to the testing room for habituation. Testing was performed during the animal's active phase under dim-light conditions. After the habituation, each rat was given compounds or vehicle before placing into the test arena for a 5 min exploration with two identical objects (E1). Scopolamine (1 mg/kg, IP in saline) and Donepezil (1.8 mg/kg, IP in saline) were given at 30 min prior to E1. BNC375 (0.01, 0.1, 1, and 10 mg/kg, PO in 25% Cremaphor) was given at 60 min prior to E1. The test arena consisted of a vinyl, opaque cylinder 32 inches in diameter with 16-inch wall. The objects used were custom-fabricated geometric shapes (cone and sphere) similar in

overall size (3 inches in height × 3 inches in diameter). Activity of the rats was video recorded and scored using visual tracking software (Cleversys). Exploration of an object was scored when the animal's nose was pointed in the direction of the object at a distance < 1 inch. Climbing over or leaning on an object is not considered to be an explorative behavior. After one hour inter-trial interval (ITI), the animals were placed back into the testing arena for 2 min of exploration (E2), which now contained one object identical to that used in E1 and another novel object. The amount of time that animals explored the novel object relative to the familiar object was the primary endpoint. In addition, total time spent exploring the objects as well as locomotion during E1 and E2 were also recorded and analyzed. Objects and locations of the object were randomly assigned and counterbalanced across groups. Animals were included in the analysis if the exploration of each object during E1 was > 1 s, total E1 exploration of both objects was > 4 s, and total exploration of both objects during E2 was > 1 s.

Object retrieval detour task

To examine the effect of BNC375 on scopolamine-induced cognitive deficits in non-human primate (NHP), 11 single-housed male rhesus monkeys (*Macaca mulatta*), 4 – 17 kg, participated as subjects in the experiment. The object retrieval detour task (ORD task) was also performed in aged male African green monkey (AGM) (17-29 years, n=8) to access the effect of BNC375 on age-associated cognitive impairments in this animal model of AD (Cramer et al., 2018). Subjects were maintained on a 12 h light:dark cycle (lights on at 06:30) with room temperatures maintained at 22 ± 2 °C. Testing was performed in each subject's home cage between 10:00 and 13:00 h. The ORD task

requires subjects to retrieve food objects (dried fruit) from a clear acrylic box with a single open plane. Sessions consisted of a fixed arrangement of “easy” (n=8) and “difficult” (n=10) trials. For easy trials, the reward was positioned either (1) inside the box, with the open plane (and reward) directly in the line of sight of the subject, (2) slightly protruding from the box with the open plane to the left or right of the subject, or (3) just inside the box with the open plane either to the left or right of the subject. The purpose of easy trials was to detect potential adverse events under drug conditions (such as motor, motivational, or visuospatial impairments). For difficult trials, the reward was placed deep inside the box opposite the open plane. Unlike easy trials, performance on difficult trials is disrupted by scopolamine and prefrontal cortex lesions and is thought to require greater attention, planning, and impulse control. A “correct” trial requires the subject to successfully reach into the open plane of the box and retrieve the reward on their first attempt. Trials were scored as “incorrect” if the subject contacted one of the solid planes of the box on the initial attempt. Subjects were not punished for incorrect reaches and all subjects eventually retrieved all rewards. A newly cleaned box was presented for every trial to eliminate visual cues from the previous handing. Prior to each trial, a barrier was placed in front of the acrylic box to prevent the subject from observing the baiting process or the position of the reward prior to the commencement of each trial. The behavioral assessments were done in real time by an experimenter blinded to the treatment.

Subjects were tested two times weekly, with at least 3 days between test sessions. Subjects were first tested under vehicle-only conditions (IM saline in the case of scopolamine and PO 30% Captisol for BNC375) until their performance stabilized. Next, the subjects were characterized on scopolamine to demonstrate sufficient impairment

compared to the vehicle baseline. Due to individual differences in sensitivity to scopolamine, each subject's "best dose" (defined as the dose that produces a > 20% deficit on difficult trials and does not significantly impact easy trial performance) was identified and subsequently replicated 2-3 times to ensure reliability. Once vehicle and scopolamine baseline performance stability were successfully established, BNC375 (0.1, 1, and 10 mg/kg, PO) characterization was initiated. Utilizing a Latin-square study design, scopolamine (or vehicle) and BNC375 (or vehicle) were administered 30 min and 2 h prior to testing, respectively. For the ORD task in AGM, BNC375 (3 mg/kg, IM) or vehicle was administered 30 min prior to testing.

Ex vivo NMR analysis of ^{13}C enrichment in brain metabolites

Adult male Sprague-Dawley rats (Charles River Laboratory, 180 – 250 g) were acclimated for one week and fasted for 12 – 18 hours prior to the experiment to ensure a fasting glucose level of around 80 to 100 mg/dL range. Animals were treated with BNC375 (10 mg/kg, PO in 25% Cremophor) or vehicle 90 min before ^{13}C-glucose (Aldrich) infusion. Tail vein catheterization was conducted under isoflurane anesthesia at 40 min prior to ^{13}C-glucose infusion. The catheter was connected to a PE50 tube filled with saline and securely taped to the tail. Ketamine (30 mg/kg, IP in saline) as a positive control was administrated at 10 min before ^{13}C-glucose infusion. ^{13}C-glucose was delivered at an exponentially decreasing rate for 8 min with the infusion rate tailored to the weight of each rat.

Eight minutes after ^{13}C-glucose infusion, rats were put into a pre-filled isoflurane chamber for ~60 s. Once anesthetized, rats were loaded into a water-jacketed rat holder and

microwaved at 5 kW for 1.7 s using a directed microwave pulse (Muromachi Microwave Fixation System) to the head to quickly arrest metabolism, allowing brain tissue to be removed without post-mortem changes (Stavinoha et al., 1973; Risa et al., 2009; Chowdhury et al., 2017). Immediately following euthanasia, the rat heads were buried in ice for about 5 min before the brains were removed, and the mPFC dissected. Whole blood (1 mL) was also collected via a cardiac puncture immediately after microwave euthanasia. Samples were then frozen on dry ice and stored at -80°C. Frozen brain tissues were then extracted in methanol : water (80:20) solution using a TissueLyser homogenizer (Bead Ruptor Elite, OMNI International NW Kennesaw, GA, USA). Samples were dried under liquid nitrogen, resuspended in PBS and pH adjusted to 7.0. Samples were freeze dried and stored until NMR analysis.

Frozen samples were re-suspended in deuterium oxide and transferred to 3 mm NMR tubes . NMR spectra of plasma and cortical extracts were acquired using a Varian 600 MHz spectrometer equipped with a ^{13}C enhanced cold probe. 1H-decoupled ^{13}C NMR signals from glutamate C4, glutamine C4, and GABA C2 were converted to μ mole units by comparison to ^{13}C NMR spectra from reference solutions acquired under identical conditions. Fractional ^{13}C enrichments in plasma glucose were determined using 1H NMR as previously described (Chowdhury et al., 2012).

Statistics

In all figures, data are presented as means ± SEM. All statistics were performed with the GraphPad Prism 6 (GraphPad Software Inc.)). A p-value of < 0.05 was considered significant. ORD task in African green monkeys was analyzed with paired t-test. ORD task

with scopolamine-induced impairment was analyzed via one-way repeated-measures analysis of variance followed by Fisher's LSD post hoc test. For other assays, one-way analysis of variance followed by Fisher's LSD post hoc tests were performed to examine group differences.

JPET Fast Forward. Published on February 24, 2020 as DOI: 10.1124/jpet.119.263483
This article has not been copyedited and formatted. The final version may differ from this version.

Results

1. Electrophysiological characterization of BNC375

BNC375 (Fig 1A) was initially discovered and optimized as a positive allosteric modulator of α7 nAChR using GH4C1 cells stably expressing human α7 nAChR (Harvey et al., 2019). Here we use IonFlux HT automated patch-clamp of human HEK α7/RIC3 cells to further characterize the effect of BNC375 on α7 nAChR. BNC375 alone does not affect channel opening to a compound concentration up to 10 μM, confirming that this compound has no intrinsic agonist activity (Fig 1B). To examine the PAM activity of BNC375, an EC_{20} concentration of ACh (40 μM) was utilized as it elicited a consistent current response and resulted in a robust assay window with adequate dynamic range. Application of EC_{20} ACh evoked a fast activating and desensitizing current (Fig 1B), which is in good agreement with the properties reported for α7 nAChR (Williams et al., 2011). Preincubation of BNC375 profoundly increased EC_{20} ACh-induced peak current amplitude by 225%, 605%, and 910% (n=7 patch-clamp recordings) at 1.11, 3.33, and 10 μM, respectively (Fig 1B, C). Notably, BNC375 has little effect on channel activation or desensitization kinetics (Fig 1B), indicating that this compound is a Type I PAM as reported by the manual patch-clamp recordings from GH4C1 cells (Harvey et al., 2019). Fig 1C shows that BNC375 potentiates EC_{20} ACh peak current amplitude in a dose-dependent manner with EC_{50}=2.64 μM and E_{max}=910%. It is worth noting that concentration higher than 10 μM was not evaluated due to low solubility of BNC375. Therefore, the E_{max} and EC_{50} were calculated based on the dose range tested but may underestimated the value.

JPET Fast Forward. Published on February 24, 2020 as DOI: 10.1124/jpet.119.263483
This article has not been copyedited and formatted. The final version may differ from this version.

In addition to charactering the effect of BNC375 on human α7 nAChR, BNC375 was further evaluated in GH4C1 cells expressing rat α7 nAChR to determine potential species difference in potency. As shown in Fig 2A, application of 3 μM BNC375 potentiated EC_{20} ACh peak current amplitude by 1386%. The concentration-response measurements of BNC375 for potentiating EC_{20} ACh-evoked peak current and net current charge (area under curve, AUC) yielded an EC_{50}=1.9 μM and 1.3 μM, respectively, suggesting the potency of BNC375 at rat α7 nAChR is closely aligned with human α7 nAChR pharmacology (Fig 2B). Figure 2C shows the concentration-response relationships for ACh in the absence and presence of 2 μM BNC375, indicating that BNC375 increased the maximal response and potency of ACh.

2. Selectivity of BNC375

BNC375 was evaluated for PAM or antagonist activity on other Cys-loop receptors with significant homology to the α7 nAChR (Table 1). The α1, α3β4, α4β2, 5-HT_{3A}, and $GABA_A$ assays used an EC_{40} concentration of their respective ligands (acetylcholine, serotonin, or GABA) to measure potentiation and antagonism, and 5-HT_{3a} antagonism was assessed using an EC_{80} concentration of serotonin. BNC375 up to 10 μM did not show PAM activity at any of the five related receptors. In the antagonist mode, BNC375 also demonstrates good selectivity over other Cys-loop receptors (Table 1).

3. Potentiation of native α7 nAChR current in hippocampal interneurons by BNC375

To assess the effects of BNC375 on native α7 nAChRs, and to confirm that the effect in native tissue is consistent with the effects observed in the cell lines over-expressing α7 receptors, BNC375 was evaluated using whole-cell voltage-clamp recordings from

morphologically and electrophysiologically identified GABAergic interneurons located within the *stratum radiatum* of rat hippocampus. The pharmacologically isolated α7 currents were induced by pressure-ejected application of ACh (2 - 5 sec) onto recorded interneurons using a glass electrode positioned ~100 μm from the recording site (Fig 3A). Brief application of 100 μM ACh evoked a fast desensitizing current which can be blocked by 200 nM of MLA, indicating the current is mediated by α7 receptors (Fig 3A). Bath application of BNC375 at 3 μM potentiated the ACh-evoked α7 currents without influencing the channel kinetics (Fig 3A). Time plot graphs demonstrate that bath application of BNC375 at 3 μM potentiated α7 peak current amplitude and mean net current charge in a time-dependent manner, which is likely due to the slow penetration of BNC375 through the hippocampal slice to the recording site (Fig 3B, C). Importantly, the effects of BNC375 can be completely blocked by bath application of 200 nM MLA (Fig 3B, C). Initially, the effects of four concentrations of BNC375 were tested upon ACh-evoked α7 currents. Thirty-minute bath application of BNC375 potentiated peak current amplitude and mean net current charge in a concentration-dependent manner (Fig 3D, E). At 3 and 10 μM, BNC375 significantly potentiated the peak current amplitude to 142.3 ± 21% ($p<0.05$) and 181.2 ± 24.5% ($p<0.01$) of baseline values, respectively (Fig 3D). BNC375 at 1, 3, and 10 μM also significantly potentiated net current charge to 168.3 ± 38.9% ($p<0.05$), 190 ± 28.8% ($p<0.05$) and 485.5 ± 181.1% ($p<0.05$) of baseline, respectively (Fig 3E). At the lowest concentration tested (0.3 μM), with a 30 min bath application of BNC375, little effect of the compound was observed. To determine if prolonged incubation may further enable the compound to access the recording site, experiments were performed with an increased application time of 60 – 90 min with 0.03

and 0.3 μM BNC375. With the prolonged application, BNC375 at 0.3 μM significantly potentiated peak current amplitude to 159.6 ± 32.7% ($p<0.05$) and net current charge to 228.3 ± 52.2% ($p<0.01$) of baseline values (Fig 3D, E).

4. BNC375 enhances LTP in hippocampal slice

α7 nAChR is highly expressed in hippocampus across multiple species, including mouse, rat, monkey, and human (Seguela et al., 1993; Breese et al., 1997; Whiteaker et al., 1999; Han et al., 2003). In addition, enhancement of synaptic transmission has been observed in rodent hippocampal slices with both α7 agonists and PAMs (Biton et al., 2007; Welsby et al., 2009; Dinklo et al., 2011). To evaluate the effects of α7 nAChR activation on long-term synaptic plasticity and compare the effects of PAMs vs an agonist, BNC375, PNU120596, and encenicline were tested for their impact on LTP induced by theta burst stimulation (TBS) (Fig 4). Extracellular field excitatory postsynaptic potentials (fEPSPs) were recorded from the *stratum radiatum* of the CA1 region in response to Schaffer collateral stimulation. Under vehicle control conditions (0.1% DMSO), LTP was induced by TBS as measured by a potentiation of the fEPSP amplitude to 119.1 ± 4.1% of baseline (Fig 4A). Although the bath application of BNC375 had no effect on on-going evoked fEPSP, the compound dose-dependently enhanced LTP (Fig 4A). At 3 and 10 μM, BNC375 significantly increased fEPSP amplitude to 139.2 ± 5.3% ($p<0.05$) and 162.5 ± 10.1% ($p<0.01$) of baseline, respectively (Fig 4A, D). In contrast, the α7 partial agonist encenicline enhanced LTP at 30 nM (151.1 ± 20.7%, $p<0.05$) but attenuated LTP at 300 nM (97.9 ± 8.6%, $p=0.1$) (Fig 4B, D). The inverted U-shaped concentration response is likely due to desensitization of α7 nAChR by sustained encenicline exposure at the high concentration, as has been shown with α7 agonists, including encenicline, in various other

preparations (Prickaerts et al., 2012; Weed et al., 2017). In addition to BNC375 and encenicline, we also evaluated the effects Type II PAM PNU120596 on hippocampal LTP. Similar to BNC375, PNU120596 enhanced LTP from 0.3 to 10 μM in a dose-dependent manner (Fig 4C, D).

5. BNC375 enhances LTP in vivo

To understand the effect of α7 PAM on long-term synaptic plasticity *in vivo*, we evaluated the impact of BNC375 on LTP in anesthetized Sprague Dawley rats. Extracellular population spike (PS) activity was recorded from the dentate gyrus of the hippocampus (Fig 5B). After 10 min of baseline recording, BNC375 (0.1, 1, or 10 mg/kg) was administrated subcutaneously 20 min prior to LTP induction. To examine if BNC375 has any effect on basal glutamatergic synaptic transmission in dentate gyrus granule cell layer, the PS amplitude at 10-20 min post vehicle or BNC375 injection was normalized to the pre-treatment baseline (Fig 5A, B). BNC375 alone has no effect on on-going PS amplitude (Fig 5C). LTP was induced by TBS of the perforant pathway with a bipolar electrode. Upon completion of LTP induction, responses were monitored for a further 60 min, and the PS amplitude at 50-60 min post LTP induction was normalized to the pre-induction baseline (10 min before LTP induction). BNC375 enhanced LTP in a dose-dependent manner (Fig 5B, D). At 10 mg/kg, BNC375 significantly potentiated LTP to 126.8% ± 4.7% of baseline (n=6, $p<0.05$ compared to the vehicle group). Plasma concentrations of BNC375 at 80 min post treatment were 0.024, 0.28, and 3.14 μM at 0.1, 1, and 10 mg/kg, respectively.

6. BNC375 reverses a scopolamine-induced deficit in rat novel object recognition

The impact of BNC375 on a scopolamine-induced deficit in rat novel object recognition was evaluated, and donepezil (1.8 mg/kg) served as a positive control (Fig 6). Scopolamine (1 mg/kg) significantly impaired recognition (44.8% ± 5.2%, $p<0.01$) as compared to the vehicle treated animals (73.1% ± 4.3%). BNC375 (0.01 to 10 mg/kg) significantly reversed the scopolamine-induced deficit at all dose levels tested (Fig 6A). The maximal effect of BNC375 at 10 mg/kg (69.9% ± 6.5%, Fig 6A) is comparable to the improvement in performance observed with donepezil (63.7% ± 3.5%, Fig 6A). None of the treatments influenced exploration time or locomotion during either E1 or E2 (Fig 6B-E). Plasma concentrations of BNC375 at 60 min post treatment were 0.0087, 0.089, 0.52, and 4.42 μM at 0.01, 0.1, 1, and 10 mg/kg dose, respectively.

7. BNC375 reverses a scopolamine-induced deficit in rhesus monkey object retrieval detour task

The non-human primate object retrieval detour (ORD) task is an assay dependent on executive function and attention, and reliant on the prefrontal cortex. Performance in the ORD task can be impaired pharmacologically by scopolamine, and this deficit can be reversed by donepezil (Vardigan et al., 2015), which is the current standard of care for AD. To examine the impact of α7 PAM on cognitive function in the rhesus monkey, BNC375 was assessed for its ability to attenuate a scopolamine-induced cognitive impairment in the ORD task (Fig 7). In animals not given scopolamine, 92.7% ± 2.4% of the cognitively-demanding difficult trials were completed correctly. Treatment with scopolamine resulted in a robust performance deficit, with only 53.6% ± 2.8% of difficult trials completed correctly ($p<0.001$ compared to vehicle alone). BNC375 at 1 and 10 mg/kg (PO, 2 h pre-treatment time) significantly attenuated the scopolamine-induced

deficit, increasing the performance to 68.2% ± 5.4% and 75.5% ± 3.7% in the difficult trials, respectively ($p<0.05$ compared to scopolamine alone, Fig 7A). BNC375 at 0.1 mg/kg had no effect on scopolamine deficit (54.6% ± 5.9%, $p=0.85$, Fig 7A). BNC375 treatment did not impact easy trial performance (Fig 7B). Total BNC375 plasma concentrations at 2 h post dosing were 0.0048, 0.028, and 0.52 μM at 0.1, 1, and 10 mg/kg, respectively. Thus, BNC375 demonstrated efficacy in the ORD task over at least 18-fold range in exposures, with no evidence of an inverted U-shaped dose-effect function. This range of efficacious exposures is larger than the approximately 3-fold range observed with donepezil in this assay, as higher doses of donepezil produce GI adverse effects that prevent animals from performing (Vardigan et al., 2015).

8. BNC375 improves cognitive function in aged African green monkeys

Aged African green monkeys (AGM) develop pathological hallmarks of AD, including plaques and neurofibrillary tangle-like structures (Cramer et al., 2018). In addition, aged AGMs demonstrate cognitive impairment which is ameliorated by donepezil, the standard care of AD (Cramer et al., 2018), suggesting that AGM may represent a novel translational animal model for AD. The effect of BNC375 in aged AGM was examined in the ORD task (Fig 8). With vehicle treatment, 32.5% ± 5.9% of the difficult trials were completed correctly by aged AGMs. BNC375 (3 mg/kg, IM) significantly ameliorated age-associated cognitive impairment, improving the performance to 58.8% ± 6.9% ($p<0.05$, Fig 8A). Aged AGMs do not display cognitive impairment in easy trials, and BNC375 has no effect on easy trials (Fig 8B). Plasma concentration of BNC375 at 30 min post treatment was 1.04 μM at 3 mg/kg dose.

9. BNC375 enhanced ^{13}C enrichment in brain metabolites

JPET Fast Forward. Published on February 24, 2020 as DOI: 10.1124/jpet.119.263483
This article has not been copyedited and formatted. The final version may differ from this version.

Activation of α7 receptor has been shown to modulate the release of various neurotransmitters, including glutamate, GABA, ACh, and dopamine. We applied ex vivo ^{13}C NMR analysis to examine the effects of BNC375 on neurotransmitter cycling in the medial prefrontal cortex (mPFC) of the rat (Chowdhury et al., 2012). A subanesthetic dose of ketamine (30 mg/kg) was evaluated as a positive control as similar treatments have been shown to have robust effects on glutamate and GABA cycling (Castner et al., 2011). Consistent with the previous findings, ketamine at 30 mg/kg had a significant impact on the percent ^{13}C enrichment for all three metabolites in the mPFC region ($P<0.05$ for glutamate-C4, GABA-C2, and glutamine-C4) (Fig 9). The effect of BNC375 was also observed in the mPFC for ^{13}C enrichment in glutamate-C4 ($P<0.05$), GABA-C2 ($p<0.05$), and a trend of enrichment in glutamine-C4 ($p=0.07$) (Fig 9). These findings demonstrate that BNC375 acutely increases mPFC glutamate, glutamine, and GABA labeling from ^{13}C glucose, suggesting neurotransmitter cycling and release are modulated by BNC375 in vivo.

10. BNC375 has no effect on cytotoxicity in vitro

High permeability to Ca^{2+} is one of the unique functional properties of α7 nAChR (Bertrand et al., 1993; Seguela et al., 1993). Excessive Ca^{2+} influx through α7 receptor may induce cytotoxicity, which has been observed in α7 expressing cell lines upon treatment with Type II α7 PAMs that reduced or abolished receptor desensitization (Ng et al., 2007; Dinklo et al., 2011; Williams et al., 2012). To determine if Type I PAM BNC375 can induce cytotoxicity and differentiate BNC375 from Type II PAMs, we evaluated BNC375, PNU120596 (Type II PAM), and the enantiomer of BNC375 (Type IIPAM) (Harvey et al., 2019) in a cytotoxicity assay with GH4C1 cells stably expressing rat α7 nAChR (Fig 10).

BNC375 up to 10 μM has no effect on cell viability of the GH4C1 cells (Fig 10A), while PNU120596 (Fig 10B) and the enantiomer of BNC375 (Fig 10C) dose-dependently reduced cell viability. Importantly, the cell deaths induced by the Type II PAMs were abolished by α7 antagonist MLA suggesting the cytotoxicity was mediated by α7 nAChR.

Discussion

Although PAMs of other Cys-loop receptors have been approved for clinical usage for decades, such as the $GABA_A$ receptor PAMs benzodiazepines, selective α7 PAMs have only recently been described in the literature (Ng et al., 2007; Timmermann et al., 2007; Dinklo et al., 2011; Hurst et al., 2013; Sahdeo et al., 2014; Post-Munson et al., 2017). The current study provides an extensive pharmacological characterization of the novel Type I α7 PAM BNC375. In both HEK cells expressing recombinant human α7 nAChRs and hippocampal interneurons expressing native rat α7 nAChRs, BNC375 potentiates ACh-evoked α7 current with little or no effect on receptor desensitization kinetics resembling the profile of Type I α7 PAMs (Ng et al., 2007; Timmermann et al., 2007). Additionally, in the absence of ACh, BNC375 has no effect on channel opening suggesting lack of endogenous agonist activity consistent with the profile of other α7 PAMs (Ng et al., 2007; Hurst et al., 2013).

Evaluating the pro-cognitive effect of BNC375 in NHPs may help us better understand the probability of success in clinical studies due to the unique translational value of NHPs (Capitanio and Emborg, 2008; Nelson and Winslow, 2009; Shively and Clarkson, 2009; Cramer et al., 2018). This may be particularly important for ligands activating α7 nAChRs given the difference in the expression pattern of α7 nAChRs in rodents as compared to higher species (Cimino et al., 1992; Breese et al., 1997; Spurden et al., 1997). For example, α7 nAChRs have been identified in reticular nuclei of the thalamus in cynomolgus macaques (Cimino et al., 1992) and in human brain (Breese et al., 1997; Spurden et al., 1997), whereas little [125I]- αBTX binding has been observed in thalamic nuclei of the rat (Clarke et al., 1985; Tribollet et al., 2004). In contrast to

reticular nuclei, high expression levels of α7 nAChRs in hippocampus have been detected across rodents, NHPs, and human (Seguela et al., 1993; Breese et al., 1997; Whiteaker et al., 1999). In addition, activation of α7 nAChR in rat hippocampus has been shown to enhance LTP both ex vivo and in vivo, indicating that BNC375 may demonstrate pro-cognitive effects in NHPs. In the present studies, we characterized BNC375 in the ORD assay in scopolamine-impaired rhesus monkeys. To our knowledge, this is the first time that an α7 Type I PAM has been evaluated in NHPs. In rhesus monkeys, BNC375 dose-dependently reversed the scopolamine-induced cognitive impairment over at least an 18-fold range in exposures. In contrast, α7 agonists, such as GTS-21, encenicline, and AZD0328, have frequently demonstrated sharp inverted U-shaped dose-effect function in NHP cognition assays (Castner et al., 2011; Cannon et al., 2013; Weed et al., 2017). For example, GTS-21 reversed ketamine-induced deficit in rhesus ORD assay only at 0.03 mg/kg but not at 0.1 or 0.01 mg/kg (Cannon et al., 2013). In a rhesus paired associated learning task, encenicline was evaluated at six doses ranging from 0.003 to 1 mg/kg, but a significant reversal of the scopolamine impairment was only observed at 0.01 mg/kg (Weed et al., 2017). These findings suggest that α7 PAMs may demonstrate efficacy over a much wider range of exposures as compared to the agonists.

In addition to the scopolamine-impaired rhesus monkeys, BNC375 was also evaluated in aged AGMs, a model that may represent an improved preclinical model of naturally occurring AD. For example, the transcriptome profile obtained from the prefrontal cortex of aged AGMs aligns with gene expression changes observed in AD brain(Cramer et al., 2018). Histologically, aged AGMs display age-related increases in Aβ plaques, and some aged animals also show evidence of naturally occurring tauopathy

(Kalinin et al., 2013; Cramer et al., 2018). Furthermore, AGMs exhibit age-related cognitive impairment in ORD assay, which can be ameliorated by the standard of AD care, donepezil (Cramer et al., 2018). The ORD task relies heavily on the function of prefrontal cortex (Eddins et al., 2014; Vardigan et al., 2015), which is where the transcriptome analysis was performed, and where the histological changes were observed in AGMs. Importantly, α7 nAChRs have been shown to reside on cholinergic and dopaminergic nerve terminals in the prefrontal cortex (Duffy et al., 2009), and in vivo microdialysis studies have reported elevated ACh and dopamine concentrations in prefrontal cortex upon α7 nAChR activation (Biton et al., 2007; Tietje et al., 2008). In the current study, aged AGMs demonstrated cognitive impairment in the ORD assay, and BNC375 at 3mg/kg significantly reversed age-related impairment to the same extent as donepezil (Cramer et al., 2018).

Ex vivo ^{13}C-NMR studies were performed here to examine the effects of BNC375 on amino acid neurotransmitter cycling and neuronal energy metabolism in rat prefrontal cortex. In this assay, ^{13}C-labeled glucose is metabolized mainly in the neuronal tricarboxylic cycle and is incorporated into neuronal glutamate and GABA, which are released at the presynaptic terminals and recycled by astrocytes, followed by conversion to glutamine (Chowdhury et al., 2012). Therefore, the NMR analysis with ^{13}C-labeled glucose can provide information on glutamate and GABA neurotransmitter cycling and neuronal metabolism. This technique has been successfully applied to characterize the physiological process underlying ketamine's rapid antidepressant-like effect in preclinical models and in human (Chowdhury et al., 2012; Abdallah et al., 2018). Here we show that BNC375, at an efficacious dose in the animal behavior studies, acutely increased ^{13}C

enrichments in mPFC glutamate, glutamine, and GABA from ^{13}C-glucose, indicating neurotransmitter cycling is enhanced by BNC375. These findings are consistent with previous in vivo microdialysis studies showing activation of α7 nAChR is associated with increased neurotransmitter release in various brain regions, including prefrontal cortex (Biton et al., 2007; Tietje et al., 2008; Livingstone et al., 2009). Over the last decade, significant progress has been made toward developing novel α7 PET tracers that bind to the orthosteric binding site (Chalon et al., 2015), such as [18F]ASEM, which has advanced to clinic to determine the target engagement of α7 agonists (Wong et al., 2014; Wong et al., 2018). However, developing an α7 PET tracer targeting the allosteric binding site has been a challenge. The ^{13}C-NMR approach could be extremely useful in demonstrating in vivo target modulation by α7 PAMs as well as the pharmacokinetic and pharmacodynamic relationship in animal models and clinical studies.

α7 nAChR is highly permeable to Ca^{2+} (Bertrand et al., 1993; Delbono et al., 1997), which is critical for its Ca^{2+}-dependent function under physiological conditions (Role and Berg, 1996; Albuquerque et al., 1997). However, accumulating evidence suggests that excessive Ca^{2+} influx through α7 receptor may perturb intracellular Ca^{2+} homeostasis and induce cytotoxicity. This has been demonstrated in a mouse model expressing α7 nAChR with “gain of function” mutation (L250T) that reduced receptor desensitization (Orr-Urtreger et al., 2000). In the homozygous mice, the mutation is associated with extensive neuronal cell death throughout cortex and is lethal at birth (Orr-Urtreger et al., 2000). In addition, Type II PAMs, but not Type I PAMs, have been shown to induce cytotoxicity in multiple cell lines expressing α7 receptor (Ng et al., 2007; Dinklo et al., 2011; Williams et al., 2012). The current study confirmed previous finding that Type II PAM PNU120596

can induce cell death in GH4C1 cells expressing α7 receptor. In addition, we compared BNC375 (type I PAM) and its enantiomer (Type II PAM) (Harvey et al., 2019) in the cytotoxicity assay. The only difference between the two molecules is the stereochemistry around the central cyclopropyl ring, which provides us an excellent tool to differentiate Type I versus Type II PAMs with regard to the impact on cell viability. As expected, the enantiomer of BNC375 induced cell death in a dose-dependent manner, while BNC375 has no effect on cell viability. Although the cytotoxicity associated with Type II PAMs needs to be further evaluated in in vivo conditions, the current findings suggest that chronic treatment of Type II PAMs may put neurons with high α7 nAChR expression levels at risk in clinical settings.

We noticed that the in vitro potency of BNC375 is in the low μM range (EC_{50} = 2.64 μM), whereas BNC375 is active in vivo at much lower exposures. For example, the minimum effective dose (MED) of BNC375 in the rat NOR assay is 0.01 mg/kg, which is associated with 0.0087 μM plasma concentration. In addition, BNC375 reversed scopolamine-induced deficit at 0.028 μM plasma exposure in the rhesus ORD assay. The dissociation between in vitro and in vivo potency has been observed with many other α7 PAMs. In fact, the in vitro potency of most α7 PAMs, such as NS1738, AVL-3288, JNJ-193942, A-867744, and RO5126946, are in the low μM range, while these compounds produce efficacy in vivo at exposures that are several orders of magnitude lower (Ng et al., 2007; Timmermann et al., 2007; Malysz et al., 2009; Dinklo et al., 2011; Sahdeo et al., 2014). For example, JNJ-1930942 was reported to potentiate α7 current in vitro with an EC50 of 1.9 μM. In contrast, JNJ-1930942 improves sensory gating in DBA/2 mice at 1.3 nM free brain exposure (Dinklo et al., 2011). Exactly how α7 PAMs produce efficacy

in vivo with such low exposure is not fully understood but this observation indicates very low levels of target engagement are sufficient to produce robust pharmacodynamic effects and this is consistent across models and species. Another possible explanation is that the potential difference in the concentrations of ACh in vitro versus in vivo may influence the potency and efficacy of BNC375. In the current study, the in vitro potency of BNC375 was determined with EC_{20} concentration of ACh, while the brain concentration of ACh at the α7 receptors is largely unknown. We have observed that the potency and efficacy of Type I PAMs can be quite sensitive to ACh concentration.

In summary, this study characterizes the in vitro and in vivo pharmacological profiles of BNC375, a novel PAM of the α7 nAChR. BNC375 potentiates ACh-induced α7 current in both cell lines recombinantly expressing human wild-type α7 nAChRs and in rat hippocampus interneurons. In hippocampal slices as well as hippocampal recording in vivo, BNC375 enhances LTP suggesting a potential benefit to cognitive processes. In vivo, BNC375 improve cognitive function in both rodents and NHPs, including the AGM model which is associated with naturally occurring AD pathology. Finally, BNC375 increases neurotransmitter cycling as demonstrated by the ^{13}C-NMR analysis, which could serve as a translational biomarker to understand target modulation in patients. These findings provide a rationale for appropriately testing a selective α7 PAM to improve cognitive function in patients with Alzheimer's disease.

Authorship Contributions

Participated in research design: Wang, Daley, Miller, Harvey, Grishin, Coles, O'Connor, Thomson, Duffy, Bell, and Uslaner.

Conducted experiments: Wang, Daley, Gakhar, Lange, Vardigan, Pearson, Zhou, Warren, Miller, Belden, Grishin, and Coles.

Performed data analysis: Wang, Daley, Gakhar, Lange, Vardigan, Pearson, Zhou, Warren, Miller, Grishin, and Coles.

Wrote or contributed to the writing of the manuscript: Wang, Daley, Miller, Warren, Bell, and Uslaner.

References

Abdallah CG, De Feyter HM, Averill LA, Jiang L, Averill CL, Chowdhury GMI, Purohit P, de Graaf RA, Esterlis I, Juchem C, Pittman BP, Krystal JH, Rothman DL, Sanacora G and Mason GF (2018) The effects of ketamine on prefrontal glutamate neurotransmission in healthy and depressed subjects. *Neuropsychopharmacology* **43**:2154-2160.

Albuquerque EX, Alkondon M, Pereira EF, Castro NG, Schrattenholz A, Barbosa CT, Bonfante-Cabarcas R, Aracava Y, Eisenberg HM and Maelicke A (1997) Properties of neuronal nicotinic acetylcholine receptors: pharmacological characterization and modulation of synaptic function. *J Pharmacol Exp Ther* **280**:1117-1136.

Bertrand D, Galzi JL, Devillers-Thiery A, Bertrand S and Changeux JP (1993) Mutations at two distinct sites within the channel domain M2 alter calcium permeability of neuronal alpha 7 nicotinic receptor. *Proc Natl Acad Sci U S A* **90**:6971-6975.

Bertrand D, Lee CH, Flood D, Marger F and Donnelly-Roberts D (2015) Therapeutic Potential of alpha7 Nicotinic Acetylcholine Receptors. *Pharmacol Rev* **67**:1025-1073.

Biton B, Bergis OE, Galli F, Nedelec A, Lochead AW, Jegham S, Godet D, Lanneau C, Santamaria R, Chesney F, Leonardon J, Granger P, Debono MW, Bohme GA, Sgard F, Besnard F, Graham D, Coste A, Oblin A, Curet O, Vige X, Voltz C, Rouquier L, Souilhac J, Santucci V, Gueudet C, Francon D, Steinberg R, Griebel G, Oury-Donat F, George P, Avenet P and Scatton B (2007) SSR180711, a novel selective alpha7 nicotinic receptor partial agonist: (1) binding and functional profile. *Neuropsychopharmacology* **32**:1-16.

Breese CR, Adams C, Logel J, Drebing C, Rollins Y, Barnhart M, Sullivan B, Demasters BK, Freedman R and Leonard S (1997) Comparison of the regional expression of nicotinic acetylcholine receptor alpha7 mRNA and [125I]-alpha-bungarotoxin binding in human postmortem brain. *J Comp Neurol* **387**:385-398.

Cannon CE, Puri V, Vivian JA, Egbertson MS, Eddins D and Uslaner JM (2013) The nicotinic alpha7 receptor agonist GTS-21 improves cognitive performance in ketamine impaired rhesus monkeys. *Neuropharmacology* **64**:191-196.

Capitanio JP and Emborg ME (2008) Contributions of non-human primates to neuroscience research. *Lancet* **371**:1126-1135.

Castner SA, Smagin GN, Piser TM, Wang Y, Smith JS, Christian EP, Mrzljak L and Williams GV (2011) Immediate and sustained improvements in working memory after selective stimulation of alpha7 nicotinic acetylcholine receptors. *Biol Psychiatry* **69**:12-18.

Chalon S, Vercouillie J, Guilloteau D, Suzenet F and Routier S (2015) PET tracers for imaging brain alpha7 nicotinic receptors: an update. *Chem Commun (Camb)* **51**:14826-14831.

Chowdhury GM, Behar KL, Cho W, Thomas MA, Rothman DL and Sanacora G (2012) (1)H-[(1)(3)C]-nuclear magnetic resonance spectroscopy measures of ketamine's effect on amino acid neurotransmitter metabolism. *Biol Psychiatry* **71**:1022-1025.

Chowdhury GM, Zhang J, Thomas M, Banasr M, Ma X, Pittman B, Bristow L, Schaeffer E, Duman RS, Rothman DL, Behar KL and Sanacora G (2017) Transiently increased glutamate cycling in rat PFC is associated with rapid onset of antidepressant-like effects. *Mol Psychiatry* **22**:120-126.

Cimino M, Marini P, Fornasari D, Cattabeni F and Clementi F (1992) Distribution of nicotinic receptors in cynomolgus monkey brain and ganglia: localization of alpha 3 subunit mRNA, alpha-bungarotoxin and nicotine binding sites. *Neuroscience* **51**:77-86.

Clarke PB, Schwartz RD, Paul SM, Pert CB and Pert A (1985) Nicotinic binding in rat brain: autoradiographic comparison of [3H]acetylcholine, [3H]nicotine, and [125I]-alpha-bungarotoxin. *J Neurosci* **5**:1307-1315.

Cramer PE, Gentzel RC, Tanis KQ, Vardigan J, Wang Y, Connolly B, Manfre P, Lodge K, Renger JJ, Zerbinatti C and Uslaner JM (2018) Aging African green monkeys manifest transcriptional, pathological, and cognitive hallmarks of human Alzheimer's disease. *Neurobiol Aging* **64**:92-106.

Deardorff WJ, Shobassy A and Grossberg GT (2015) Safety and clinical effects of EVP-6124 in subjects with Alzheimer's disease currently or previously receiving an acetylcholinesterase inhibitor medication. *Expert Rev Neurother* **15**:7-17.

Delbono O, Gopalakrishnan M, Renganathan M, Monteggia LM, Messi ML and Sullivan JP (1997) Activation of the recombinant human alpha 7 nicotinic acetylcholine receptor significantly raises intracellular free calcium. *J Pharmacol Exp Ther* **280**:428-438.

Dinklo T, Shaban H, Thuring JW, Lavreysen H, Stevens KE, Zheng L, Mackie C, Grantham C, Vandenberk I, Meulders G, Peeters L, Verachtert H, De Prins E and Lesage AS (2011) Characterization of 2-[[4-fluoro-3-(trifluoromethyl)phenyl]amino]-4-(4-pyridinyl)-5-thiazolemethanol (JNJ-1930942), a novel positive allosteric modulator of the {alpha}7 nicotinic acetylcholine receptor. *J Pharmacol Exp Ther* **336**:560-574.

Duffy AM, Zhou P, Milner TA and Pickel VM (2009) Spatial and intracellular relationships between the alpha7 nicotinic acetylcholine receptor and the vesicular acetylcholine transporter in the prefrontal cortex of rat and mouse. *Neuroscience* **161**:1091-1103.

Eddins D, Hamill TG, Puri V, Cannon CE, Vivian JA, Sanabria-Bohorquez SM, Cook JJ, Morrow JA, Thomson F and Uslaner JM (2014) The relationship between glycine transporter 1 occupancy and the effects of the glycine transporter 1 inhibitor RG1678 or ORG25935 on object retrieval performance in scopolamine impaired rhesus monkey. *Psychopharmacology (Berl)* **231**:511-519.

Freedman R, Hall M, Adler LE and Leonard S (1995) Evidence in postmortem brain tissue for decreased numbers of hippocampal nicotinic receptors in schizophrenia. *Biol Psychiatry* **38**:22-33.

Gee KW, Olincy A, Kanner R, Johnson L, Hogenkamp D, Harris J, Tran M, Edmonds SA, Sauer W, Yoshimura R, Johnstone T and Freedman R (2017) First in human trial of a type I positive allosteric modulator of alpha7-nicotinic acetylcholine receptors: Pharmacokinetics, safety, and evidence for neurocognitive effect of AVL-3288. *J Psychopharmacol* **31**:434-441.

Guan ZZ, Zhang X, Ravid R and Nordberg A (2000) Decreased protein levels of nicotinic receptor subunits in the hippocampus and temporal cortex of patients with Alzheimer's disease. *J Neurochem* **74**:237-243.

Han ZY, Zoli M, Cardona A, Bourgeois JP, Changeux JP and Le Novere N (2003) Localization of [3H]nicotine, [3H]cytisine, [3H]epibatidine, and [125I]alpha-bungarotoxin binding sites in the brain of Macaca mulatta. *J Comp Neurol* **461**:49-60.

Harvey AJ, Avery TD, Schaeffer L, Joseph C, Huff BC, Singh R, Morice C, Giethlen B, Grishin AA, Coles CJ, Kolesik P, Wagner S, Andriambeloson E, Huyard B, Poiraud E, Paul D and O'Connor SM (2019) Discovery of BNC375, a Potent, Selective, and Orally Available Type I Positive Allosteric Modulator of alpha7 nAChRs. *ACS Med Chem Lett* **10**:754-760.

Huang M, Felix AR, Kwon S, Lowe D, Wallace T, Santarelli L and Meltzer HY (2014) The alpha-7 nicotinic receptor partial agonist/5-HT3 antagonist RG3487 enhances cortical and hippocampal dopamine and acetylcholine release. *Psychopharmacology (Berl)* **231**:2199-2210.

Hurst R, Rollema H and Bertrand D (2013) Nicotinic acetylcholine receptors: from basic science to therapeutics. *Pharmacol Ther* **137**:22-54.

Kadir A, Almkvist O, Wall A, Langstrom B and Nordberg A (2006) PET imaging of cortical 11C-nicotine binding correlates with the cognitive function of attention in Alzheimer's disease. *Psychopharmacology (Berl)* **188**:509-520.

Kalinin S, Willard SL, Shively CA, Kaplan JR, Register TC, Jorgensen MJ, Polak PE, Rubinstein I and Feinstein DL (2013) Development of amyloid burden in African Green monkeys. *Neurobiol Aging* **34**:2361-2369.

Keller JJ, Keller AB, Bowers BJ and Wehner JM (2005) Performance of alpha7 nicotinic receptor null mutants is impaired in appetitive learning measured in a signaled nose poke task. *Behav Brain Res* **162**:143-152.

Koranda JL, Cone JJ, McGehee DS, Roitman MF, Beeler JA and Zhuang X (2014) Nicotinic receptors regulate the dynamic range of dopamine release in vivo. *J Neurophysiol* **111**:103-111.

Le Pichon JB, Yu S, Kibiryeva N, Graf WD and Bittel DC (2013) Genome-wide gene expression in a patient with 15q13.3 homozygous microdeletion syndrome. *Eur J Hum Genet* **21**:1093-1099.

Livingstone PD, Srinivasan J, Kew JN, Dawson LA, Gotti C, Moretti M, Shoaib M and Wonnacott S (2009) alpha7 and non-alpha7 nicotinic acetylcholine receptors modulate dopamine release in vitro and in vivo in the rat prefrontal cortex. *Eur J Neurosci* **29**:539-550.

Malysz J, Gronlien JH, Anderson DJ, Hakerud M, Thorin-Hagene K, Ween H, Wetterstrand C, Briggs CA, Faghih R, Bunnelle WH and Gopalakrishnan M (2009) In vitro pharmacological characterization of a novel allosteric modulator of alpha 7 neuronal acetylcholine receptor, 4-(5-(4-chlorophenyl)-2-methyl-3-propionyl-1H-pyrrol-1-yl)benzenesulfonamide (A-867744), exhibiting unique pharmacological profile. *J Pharmacol Exp Ther* **330**:257-267.

Nelson EE and Winslow JT (2009) Non-human primates: model animals for developmental psychopathology. *Neuropsychopharmacology* **34**:90-105.

Ng HJ, Whittemore ER, Tran MB, Hogenkamp DJ, Broide RS, Johnstone TB, Zheng L, Stevens KE and Gee KW (2007) Nootropic alpha7 nicotinic receptor allosteric modulator derived from GABAA receptor modulators. *Proc Natl Acad Sci U S A* **104**:8059-8064.

Orr-Urtreger A, Broide RS, Kasten MR, Dang H, Dani JA, Beaudet AL and Patrick JW (2000) Mice homozygous for the L250T mutation in the alpha7 nicotinic acetylcholine receptor show increased neuronal apoptosis and die within 1 day of birth. *J Neurochem* **74**:2154-2166.

Perkins KA, Roy Chengappa KN, Karelitz JL, Boldry MC, Michael V, Herb T, Gannon J, Brar J, Ford L, Rassnick S and Brunzell DH (2018) Initial Cross-Over Test of A Positive Allosteric Modulator of Alpha-7 Nicotinic Receptors to Aid Cessation in Smokers With Or Without Schizophrenia. *Neuropsychopharmacology* **43**:1334-1342.

Pichat P, Bergis OE, Terranova JP, Urani A, Duarte C, Santucci V, Gueudet C, Voltz C, Steinberg R, Stemmelin J, Oury-Donat F, Avenet P, Griebel G and Scatton B (2007) SSR180711, a novel selective alpha7 nicotinic receptor partial agonist: (II) efficacy in experimental models predictive of activity against cognitive symptoms of schizophrenia. *Neuropsychopharmacology* **32**:17-34.

Post-Munson DJ, Pieschl RL, Molski TF, Graef JD, Hendricson AW, Knox RJ, McDonald IM, Olson RE, Macor JE, Weed MR, Bristow LJ, Kiss L, Ahlijanian MK and Herrington J (2017) B-973, a novel piperazine positive allosteric modulator of the alpha7 nicotinic acetylcholine receptor. *Eur J Pharmacol* **799**:16-25.

Prickaerts J, van Goethem NP, Chesworth R, Shapiro G, Boess FG, Methfessel C, Reneerkens OA, Flood DG, Hilt D, Gawryl M, Bertrand S, Bertrand D and Konig G (2012) EVP-6124, a novel and selective alpha7 nicotinic acetylcholine receptor partial agonist, improves memory performance by potentiating the acetylcholine response of alpha7 nicotinic acetylcholine receptors. *Neuropharmacology* **62**:1099-1110.

Rezvani AH, Kholdebarin E, Brucato FH, Callahan PM, Lowe DA and Levin ED (2009) Effect of R3487/MEM3454, a novel nicotinic alpha7 receptor partial agonist and 5-HT3 antagonist on sustained attention in rats. *Prog Neuropsychopharmacol Biol Psychiatry* **33**:269-275.

Risa O, Melo TM and Sonnewald U (2009) Quantification of amounts and (13)C content of metabolites in brain tissue using high- resolution magic angle spinning (13)C NMR spectroscopy. *NMR Biomed* **22**:266-271.

Role LW and Berg DK (1996) Nicotinic receptors in the development and modulation of CNS synapses. *Neuron* **16**:1077-1085.

Sahdeo S, Wallace T, Hirakawa R, Knoflach F, Bertrand D, Maag H, Misner D, Tombaugh GC, Santarelli L, Brameld K, Milla ME and Button DC (2014) Characterization of RO5126946, a Novel alpha7 nicotinic acetylcholine receptor-positive allosteric modulator. *J Pharmacol Exp Ther* **350**:455-468.

Seguela P, Wadiche J, Dineley-Miller K, Dani JA and Patrick JW (1993) Molecular cloning, functional properties, and distribution of rat brain alpha 7: a nicotinic cation channel highly permeable to calcium. *J Neurosci* **13**:596-604.

Sharp AJ, Mefford HC, Li K, Baker C, Skinner C, Stevenson RE, Schroer RJ, Novara F, De Gregori M, Ciccone R, Broomer A, Casuga I, Wang Y, Xiao C, Barbacioru C, Gimelli G, Bernardina BD, Torniero C, Giorda R, Regan R, Murday V, Mansour S, Fichera M, Castiglia L, Failla P, Ventura M, Jiang Z, Cooper GM, Knight SJ, Romano C, Zuffardi O, Chen C, Schwartz CE and Eichler EE (2008) A recurrent 15q13.3 microdeletion syndrome associated with mental retardation and seizures. *Nat Genet* **40**:322-328.

Shively CA and Clarkson TB (2009) The unique value of primate models in translational research. Nonhuman primate models of women's health: introduction and overview. *Am J Primatol* **71**:715-721.

Spurden DP, Court JA, Lloyd S, Oakley A, Perry R, Pearson C, Pullen RG and Perry EK (1997) Nicotinic receptor distribution in the human thalamus: autoradiographical localization of [3H]nicotine and [125I] alpha-bungarotoxin binding. *J Chem Neuroanat* **13**:105-113.

Stavinoha WB, Weintraub ST and Modak AT (1973) The use of microwave heating to inactivate cholinesterase in the rat brain prior to analysis for acetylcholine. *J Neurochem* **20**:361-371.

Tietje KR, Anderson DJ, Bitner RS, Blomme EA, Brackemeyer PJ, Briggs CA, Browman KE, Bury D, Curzon P, Drescher KU, Frost JM, Fryer RM, Fox GB, Gronlien JH, Hakerud M, Gubbins EJ, Halm S, Harris R, Helfrich RJ, Kohlhaas KL, Law D, Malysz J, Marsh KC, Martin RL, Meyer MD, Molesky AL, Nikkel AL, Otte S, Pan L, Puttfarcken PS, Radek RJ, Robb HM, Spies E, Thorin-Hagene K, Waring JF, Ween H, Xu H, Gopalakrishnan M and Bunnelle WH (2008) Preclinical characterization of A-582941: a novel alpha7 neuronal nicotinic receptor agonist with broad spectrum cognition-enhancing properties. *CNS Neurosci Ther* **14**:65-82.

Timmermann DB, Gronlien JH, Kohlhaas KL, Nielsen EO, Dam E, Jorgensen TD, Ahring PK, Peters D, Holst D, Christensen JK, Malysz J, Briggs CA, Gopalakrishnan M and Olsen GM (2007) An allosteric modulator of the alpha7 nicotinic acetylcholine receptor possessing cognition-enhancing properties in vivo. *J Pharmacol Exp Ther* **323**:294-307.

Tribollet E, Bertrand D, Marguerat A and Raggenbass M (2004) Comparative distribution of nicotinic receptor subtypes during development, adulthood and aging: an autoradiographic study in the rat brain. *Neuroscience* **124**:405-420.

Vardigan JD, Cannon CE, Puri V, Dancho M, Koser A, Wittmann M, Kuduk SD, Renger JJ and Uslaner JM (2015) Improved cognition without adverse effects: novel M1 muscarinic potentiator compares favorably to donepezil and xanomeline in rhesus monkey. *Psychopharmacology (Berl)* **232**:1859-1866.

Weed MR, Polino J, Signor L, Bookbinder M, Keavy D, Benitex Y, Morgan DG, King D, Macor JE, Zaczek R, Olson R and Bristow LJ (2017) Nicotinic alpha 7 receptor agonists EVP-6124 and BMS-933043, attenuate scopolamine-induced deficits in visuo-spatial paired associates learning. *PLoS One* **12**:e0187609.

Welsby PJ, Rowan MJ and Anwyl R (2009) Intracellular mechanisms underlying the nicotinic enhancement of LTP in the rat dentate gyrus. *Eur J Neurosci* **29**:65-75.

Wevers A, Burghaus L, Moser N, Witter B, Steinlein OK, Schutz U, Achnitz B, Krempel U, Nowacki S, Pilz K, Stoodt J, Lindstrom J, De Vos RA, Jansen Steur EN and Schroder H (2000) Expression of

nicotinic acetylcholine receptors in Alzheimer's disease: postmortem investigations and experimental approaches. *Behav Brain Res* **113**:207-215.

Whiteaker P, Davies AR, Marks MJ, Blagbrough IS, Potter BV, Wolstenholme AJ, Collins AC and Wonnacott S (1999) An autoradiographic study of the distribution of binding sites for the novel alpha7-selective nicotinic radioligand [3H]-methyllycaconitine in the mouse brain. *Eur J Neurosci* **11**:2689-2696.

Williams DK, Peng C, Kimbrell MR and Papke RL (2012) Intrinsically low open probability of alpha7 nicotinic acetylcholine receptors can be overcome by positive allosteric modulation and serum factors leading to the generation of excitotoxic currents at physiological temperatures. *Mol Pharmacol* **82**:746-759.

Williams DK, Wang J and Papke RL (2011) Investigation of the molecular mechanism of the alpha7 nicotinic acetylcholine receptor positive allosteric modulator PNU-120596 provides evidence for two distinct desensitized states. *Mol Pharmacol* **80**:1013-1032.

Wong DF, Kuwabara H, Horti AG, Roberts JM, Nandi A, Cascella N, Brasic J, Weerts EM, Kitzmiller K, Phan JA, Gapasin L, Sawa A, Valentine H, Wand G, Mishra C, George N, McDonald M, Lesniak W, Holt DP, Azad BB, Dannals RF, Kem W, Freedman R and Gjedde A (2018) Brain PET Imaging of alpha7-nAChR with [18F]ASEM: Reproducibility, Occupancy, Receptor Density, and Changes in Schizophrenia. *Int J Neuropsychopharmacol* **21**:656-667.

Wong DF, Kuwabara H, Pomper M, Holt DP, Brasic JR, George N, Frolov B, Willis W, Gao Y, Valentine H, Nandi A, Gapasin L, Dannals RF and Horti AG (2014) Human brain imaging of alpha7 nAChR with [(18)F]ASEM: a new PET radiotracer for neuropsychiatry and determination of drug occupancy. *Mol Imaging Biol* **16**:730-738.

Young JW, Crawford N, Kelly JS, Kerr LE, Marston HM, Spratt C, Finlayson K and Sharkey J (2007) Impaired attention is central to the cognitive deficits observed in alpha 7 deficient mice. *Eur Neuropsychopharmacol* **17**:145-155.

Footnotes

Funding: This work was funded entirely by Merck & Co., Inc. and Bionomics Limited.

Person to receive reprint request:

Xiaohai Wang

Department of Neuroscience Research, Merck & Co., Inc.,

770 Sumneytown Pike, WP14-3393, West Point, PA 19486

Tel: 215-6521085

Email: xiaohai_wang@merck.com

Xiaohai Wang[1], Christopher Daley[1], Vanita Gakhar[1], Henry Lange[1], Joshua D. Vardigan[1], Michelle Pearson[1], Xiaoping Zhou[1], Lee Warren[1], Corin O. Miller[1], Michelle Belden[1], Andrew J. Harvey[2, 3], Anton A. Grishin[2], Carolyn J. Coles[2], Susan M. O'Connor[2], Fiona Thomson[1, 4], Joseph L. Duffy[1], Ian M. Bell[1], Jason M. Uslaner[1]

1. Merck & Co., Inc., 2015 Galloping Hill Road, Kenilworth, NJ 07033, USA
2. Bionomics Limited, 31 Dalgleish Street, Thebarton, SA-5031, Australia
3. Current address: UniQuest Pty Ltd., Level 7, General Purpose South Building, Staff House Road, Brisbane, QLD-4072, Australia
4. Current address: Institute of Cancer Sciences, University of Glasgow, Glasgow G61 1QH, UK

Legends for Figures

Figure 1. IonFlux HT automated patch-clamp of HEK human α7/RIC3 cell line reveals that BNC375 potentiates ACh-evoked α7 currents in a dose-dependent manner. (A) Chemical structure of BNC375. (B) Representative traces showing the effects of BNC375 α7 currents on the 1-sec application of EC50 ACh-evoked. BNC375 alone has no effect on α7 currents. (C) BNC375 dose-dependently potentiates acetylcholine-evoked α7 peak currents up to 910% with an EC_{50} of approximately 2.6 μM (n = 7).

Figure 2. BNC375 potentiates ACh-evoked α7 currents in GH4C1 cells stably expressing rat α7 nAChR. (A) Representative traces of α7 currents evoked by EC_{20} ACh in the absence or presence 3 μM BNC375. (B) Concentration-response relationship showing potentiation of ACh peak current and net current charge (area under curve, AUC) by BNC375. For peak current potentiation, EC_{50} = 1.9 μM, n_H = 1.6, Emax = 1572%. For AUC potentiation, EC_{50} = 1.3 μM, n_H = 1.6, Emax = 2616%. (C) Effects of BNC375 on the ACh concentration-response curve. Plot of the peak ACh-evoked currents by ACh alone (EC_{50} = 127.7, n_H = 1.8) and in the presence of 2 μM BNC375 (EC_{50} = 14.5 μM, n_H =1.7, data normalized to EC_{100} ACh current).

Figure 3. Effects of BNC375 on ACh-evoked α7 current in rat hippocampal interneurons. (A) Representative traces of pharmacologically isolated α7 current evoked by brief application of 100 μM ACh in stratum radiatum interneurons showing potentiation effect of 3 μM BNC375 and inhibition of the current upon co-application of 200 nM MLA. (B-C)

Example time plots showing the effects of 3 μM BNC375 on normalized peak current amplitude (B) and net current charge (C). Application of 200 nM MLA abolished the ACh-evoked current. (D-E) Dose-dependent effects of BNC375 on peak amplitude (D) and net current charge (E) of ACh-evoked α7 current in hippocampal interneurons. (* $p<0.05$, ** $p<0.01$, n=5-10/group).

Figure 4. Effects of BNC375 and encenicline on LTP in rat hippocampal slices. (A-C) Time plots showing normalized fEPSP amplitude in the presence of 0.1% DMSO and 0.3 – 10 μM BNC375 (A), 0.3 – 300 nM of encenicline (B), and 0.3 – 10 μM PNU120596 (C). Red lines indicate the duration of 0.1% DMSO or test compounds administration. Arrows indicate the onset of TBS. (D) BNC375 and PNU120596 enhance LTP in a dose-dependent manner, whereas encenicline enhances LTP at low concentrations but attenuates LTP at a high concentration (* $p<0.05$, ** $p<0.01$ as compared to the 0.1% DMSO group, n=6-8/group).

Figure 5. Effects of BNC375 on TBS-induced LTP recorded from the rat dentate gyrus in vivo. (A) Experimental design illustrating the duration of population spike recording and the onset of BNC375 or vehicle administration and TBS stimulation. (B) Time plots showing the effect of BNC375 on normalized pop-spike amplitude post TBS stimulation. (C) BNC375 alone has no effect on on-going population spike amplitude prior to TBS. (D) BNC375 (0.1 – 10 mg/kg, SC) dose-dependently potentiated TBS-induced LTP recorded from the rat dentate gyrus in vivo (n = 6/group, *$p<0.05$).

Figure 6. Effect of BNC375 and donepezil (Don, 1.8 mg/kg, IP) on a scopolamine-induced impairment in novel object recognition in rats. (A) Percentage exploration of the novel object during the second exposure (* $p < 0.05$ compared to the vehicle-scopolamine group, n=7-11/group). (B-C) BNC375 and donepezil administration has no effect on object exploration time during the first exposure E1 (B) and the second exposure E2 (C). (D-E) BNC375 and donepezil treatment does not influence locomotion during E1 (D) and E2 (E).

Figure 7. Effect of BNC375 on scopolamine-induced impairment in an object retrieval detour task in the rhesus monkey. (A) BNC375 dose-dependently reversed scopolamine-induced impairment in the difficult trials. (B) BNC375 has no effect on easy trials. (* $p<0.05$ compared to the scopolamine alone group, n=11/group).

Figure 8. Effect of BNC375 on an object retrieval detour task in aged African green monkeys. BNC375 at 3 mg/kg significantly improved performance in the difficult trials (A), but not in the easy trials (B). (* $p<0.05$, n=8/group).

Figure 9. Effect of BNC375 and ketamine on ^{13}C enrichment of brain metabolites in rat medial prefrontal cortex following ^{13}C glucose infusion. ^{13}C enrichment of glutamate – C4

(A), glutamine – C4 (B), and GABA – C2 (C) following administration of ketamine (30 mg/kg, IP) and BNC375 (10 mg/kg, PO). (* $p < 0.05$, ** $p<0.01$, n=12/group)

Figure 10. Cytotoxicity assay comparing the effects of Type I and Type II α7 PAMs on cell viability in vitro. GH4C1 cells expressing rat α7 nAChR were incubated with BNC375 (A), PNU-120596 (B), the enantiomer of BNC375 (C), or positive control 50% DMSO for 2 h. Cytotoxicity was determined by XTT-based assay. PNU-120596 and the enantiomer of BNC375, but not BNC375, dose-dependently reduced cell viability. Application of MLA (10 μM) abolished the cytotoxicity induced by PNU-120596 and the enantiomer of BNC375. (*$p<0.05$, n=3-4/group compared with the vehicle group)

JPET Fast Forward. Published on February 24, 2020 as DOI: 10.1124/jpet.119.263483
This article has not been copyedited and formatted. The final version may differ from this version.

Tables

Table 1. Selectivity of BNC375 against other Cys-loop family of ligand-gated ion channels

Cys-loop Receptor	PAM EC50 μM	Antagonist IC50 μM
nAChR α1	> 10 μM	> 10 μM
nAChR α3β4	> 10 μM	4.70 μM
nAChR α4β2	> 10 μM	> 10 μM
nAChR α7	2.64 μM	> 10 μM
$GABA_A$	> 10 μM	> 10 μM
$5\text{-}HT3_A$	ND	6.47 μM

JPET Fast Forward. Published on February 24, 2020 as DOI: 10.1124/jpet.119.263483
This article has not been copyedited and formatted. The final version may differ from this version.

Figures

Fig.1

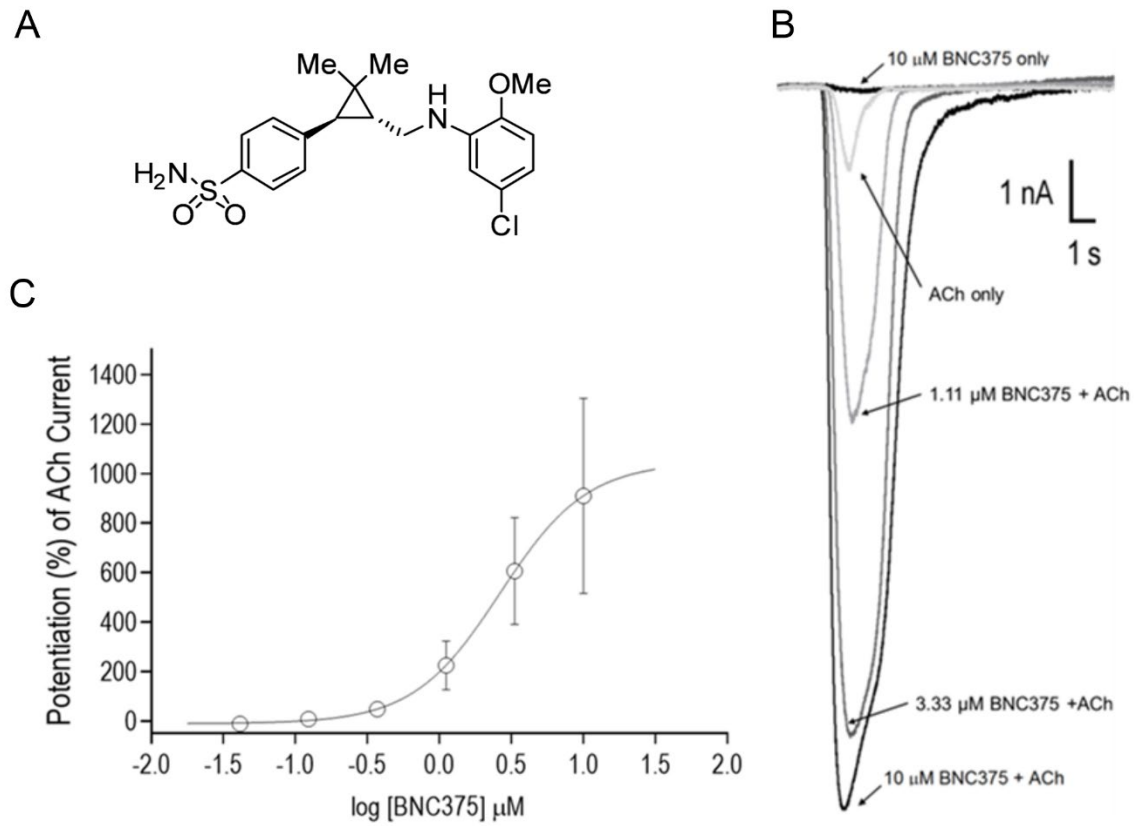

JPET Fast Forward. Published on February 24, 2020 as DOI: 10.1124/jpet.119.263483
This article has not been copyedited and formatted. The final version may differ from this version.

Fig. 2

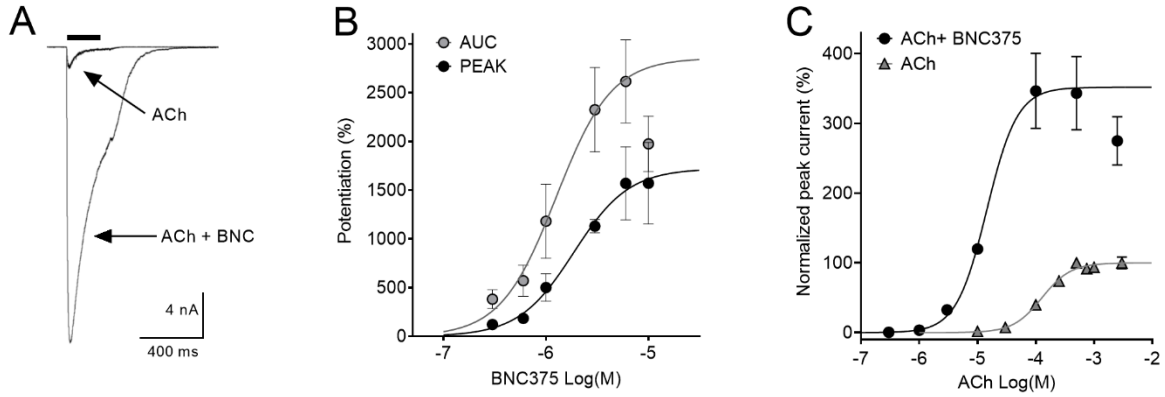

JPET Fast Forward. Published on February 24, 2020 as DOI: 10.1124/jpet.119.263483
This article has not been copyedited and formatted. The final version may differ from this version.

Fig. 3

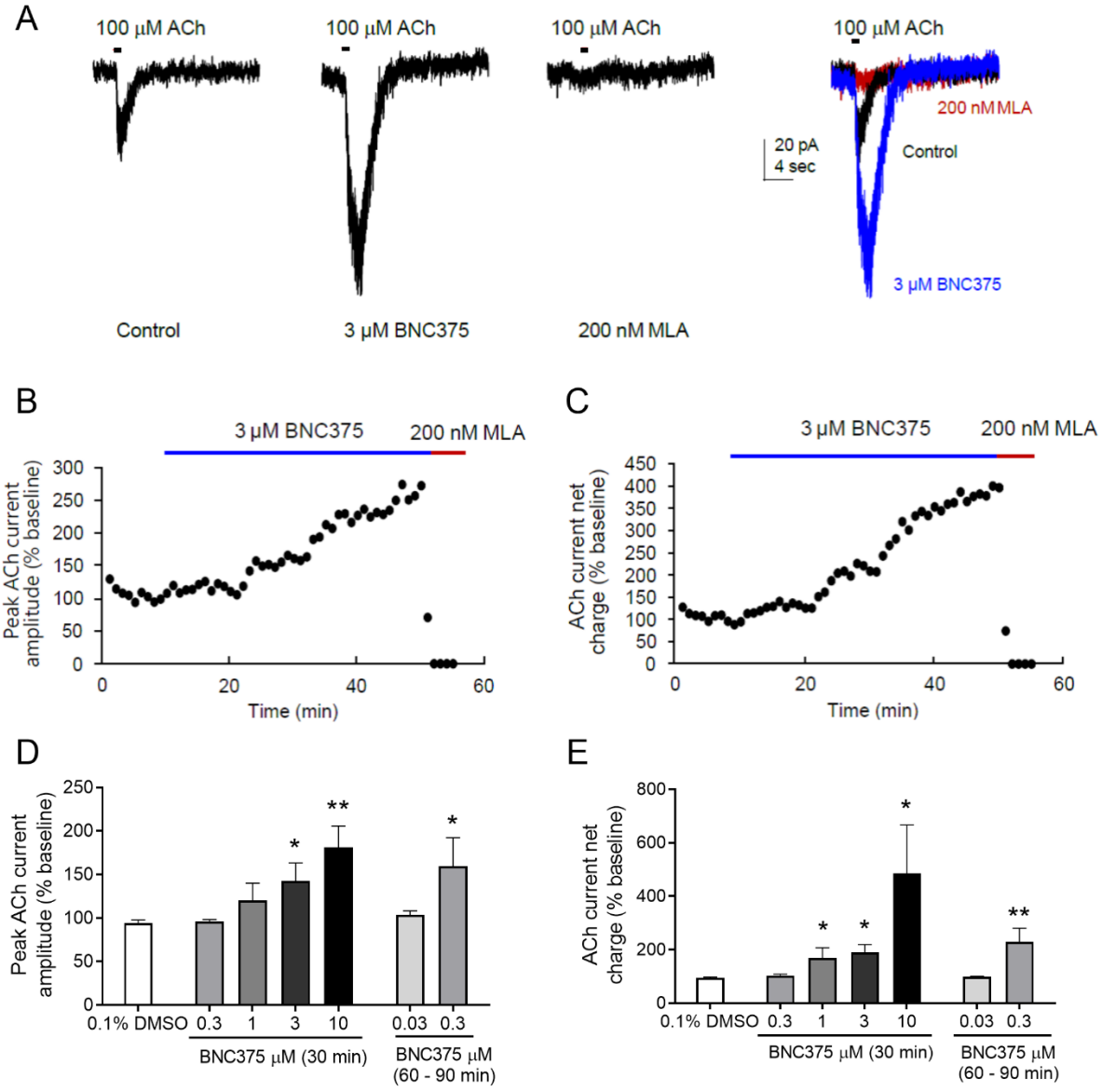

JPET Fast Forward. Published on February 24, 2020 as DOI: 10.1124/jpet.119.263483
This article has not been copyedited and formatted. The final version may differ from this version.

Fig. 4

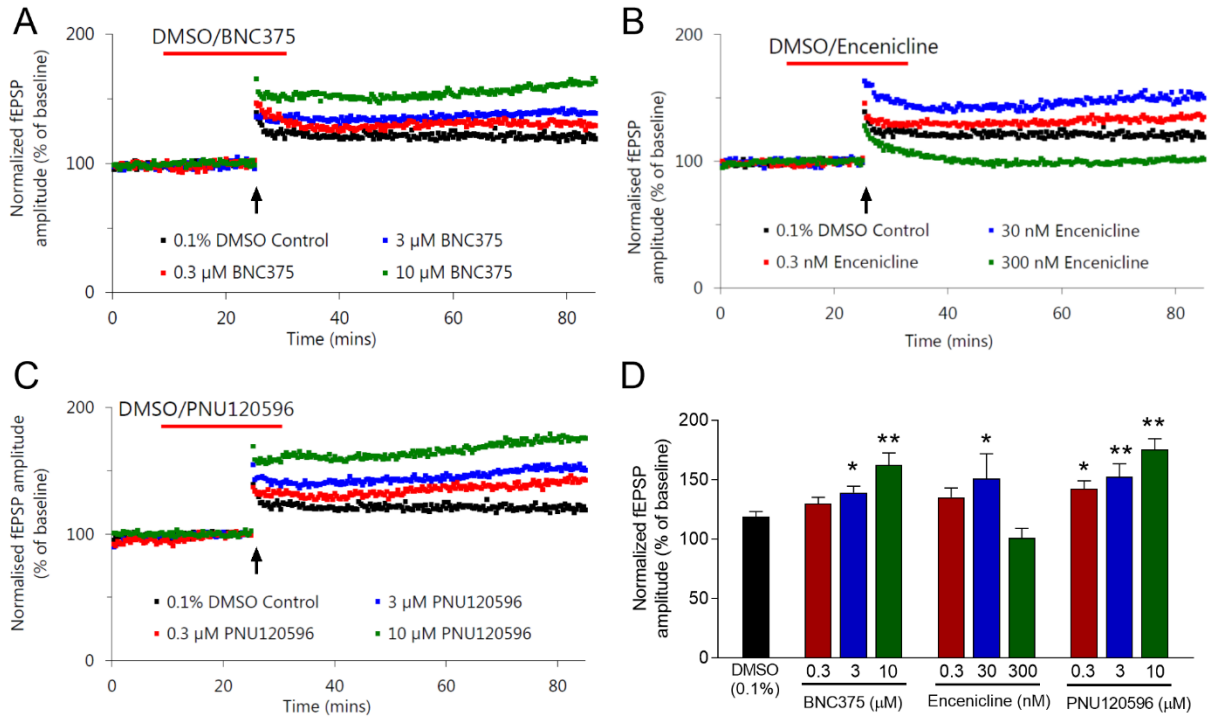

JPET Fast Forward. Published on February 24, 2020 as DOI: 10.1124/jpet.119.263483
This article has not been copyedited and formatted. The final version may differ from this version.

Fig. 5

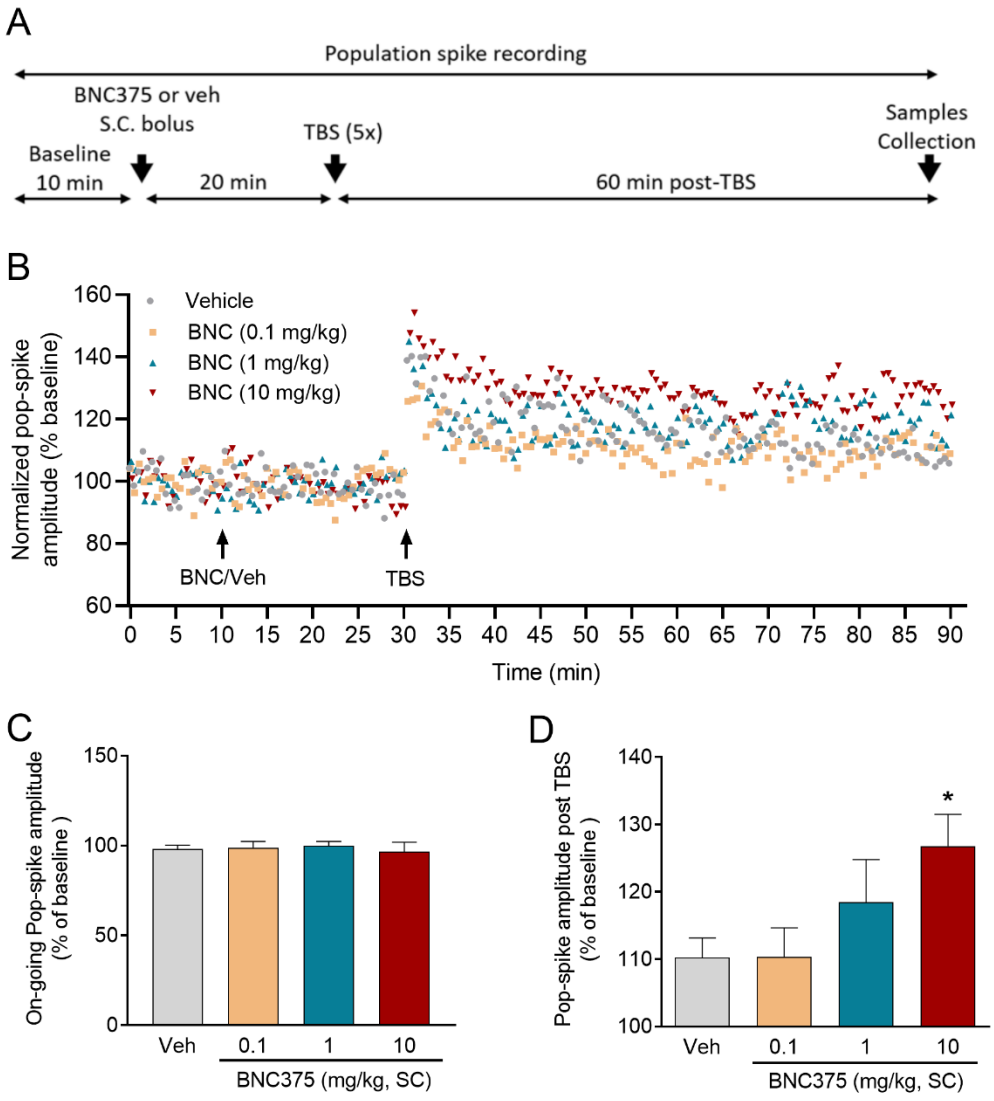

JPET Fast Forward. Published on February 24, 2020 as DOI: 10.1124/jpet.119.263483
This article has not been copyedited and formatted. The final version may differ from this version.

Fig. 6

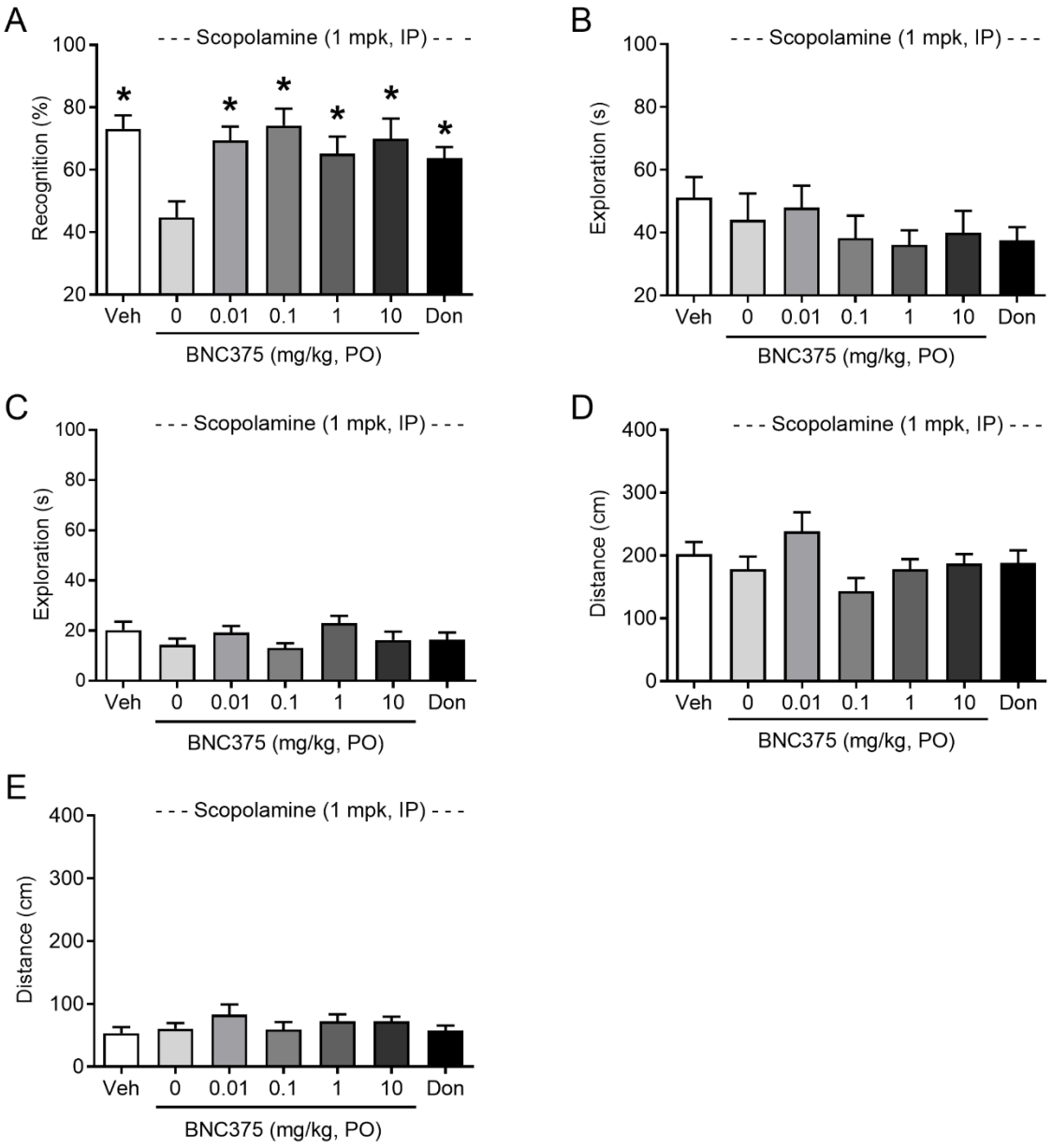

JPET Fast Forward. Published on February 24, 2020 as DOI: 10.1124/jpet.119.263483
This article has not been copyedited and formatted. The final version may differ from this version.

Fig. 7

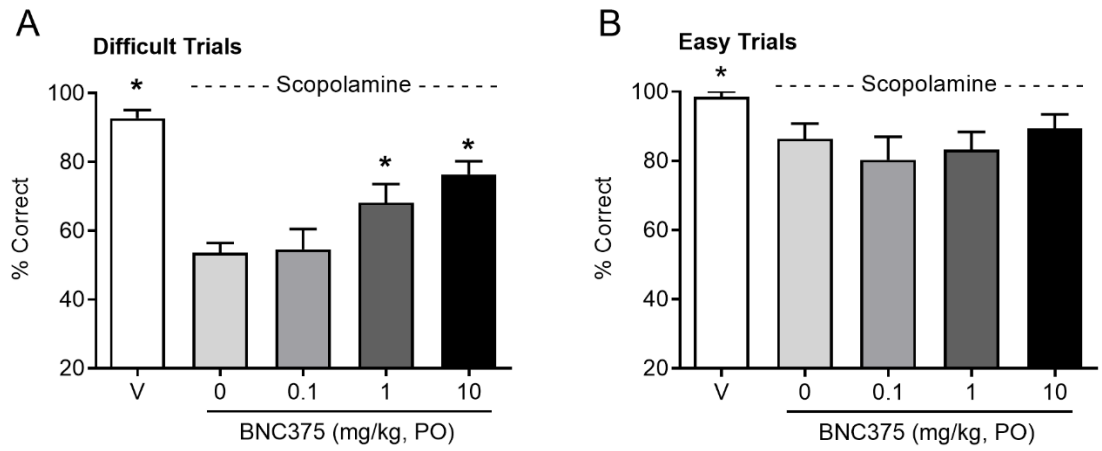

JPET Fast Forward. Published on February 24, 2020 as DOI: 10.1124/jpet.119.263483
This article has not been copyedited and formatted. The final version may differ from this version.

Fig. 8

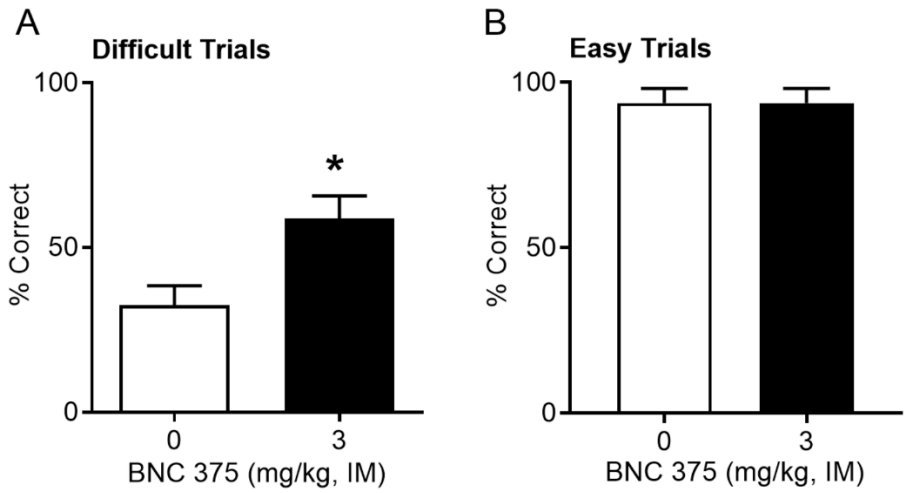

JPET Fast Forward. Published on February 24, 2020 as DOI: 10.1124/jpet.119.263483
This article has not been copyedited and formatted. The final version may differ from this version.

Fig. 9

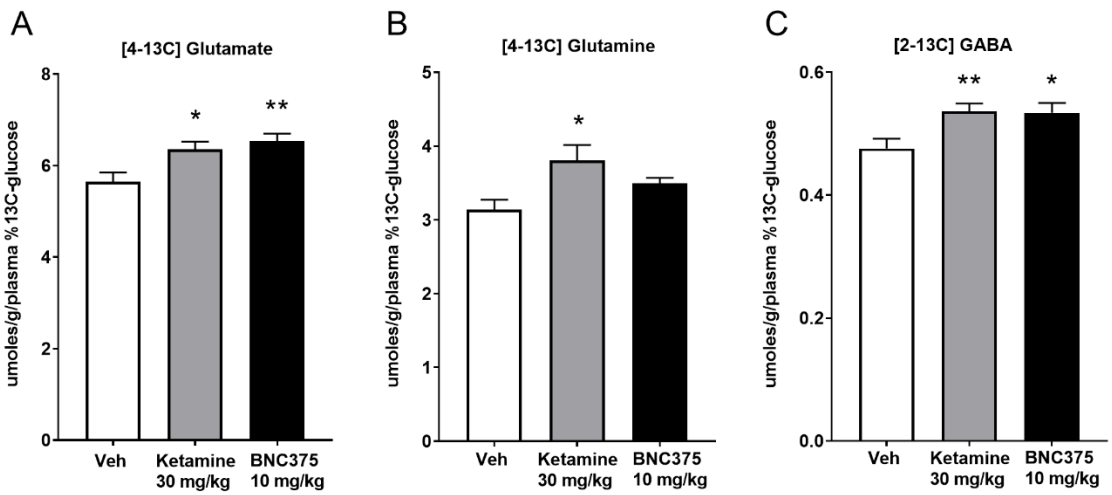

JPET Fast Forward. Published on February 24, 2020 as DOI: 10.1124/jpet.119.263483
This article has not been copyedited and formatted. The final version may differ from this version.

Fig. 10